

TECHNICAL UNIVERSITY OF CRETE
ELECTRICAL AND COMPUTER ENGINEERING
DEPARTMENT

**Energy efficiency and quality
control of polymer extrusion
process based on intelligent
control techniques**

Diploma Thesis by:
Maria Bitirini

Supervisor:
Prof. George Stavrakakis
Prof. Kostas Kalaitzakis
Co-Supervisor:
Dr Eleftheria Sergaki



Acknowledgments

I take this opportunity to express my deep gratitude to my research and scientific advisor, Dr Eleftheria Sergaki, for her support, encouragement and availability. I am indebted to her for the opportunity to work in the regression analysis modeling and control methods in polymer extrusion.

I would like to thank Prof George Stavrakakis and Prof Kostas Kalaitzakis for their support to this thesis.

The contribution and support from my family throughout my studies all these years.

Last but not least, my gratitude goes to Tasos for all the support during my studies in Technical University of Crete and without whom this work would not have been materialised.

Abstract

Polymer extrusion, in which a polymer is melted and conveyed to a mould or die, forms the basis of most polymer processing techniques. Product quality is a major issue of concern of processors. The product quality in polymer extrusion process is largely depended on melt viscosity.

The real time monitoring and control of viscosity is a difficult procedure due to the plant non-linearities. In this thesis, a model based fuzzy control framework is proposed. The fuzzy controller output is the convenient velocity regulation based on an error signal input, which is generated by real time measured velocity and the real time predicted velocity by the temperature sensors readings. The velocity model prediction is a non-linear dynamic model, with four inputs for its prediction (i.e. barrels points temperatures). The velocity regulation achieves die melt temperature stabilization (eliminates the melt temperature variance) by succeeding the desired die melt average temperature. This novel feedback structure enables the online adaptability of the velocity model in response to modeling errors and disturbances, hence producing a reliable velocity estimate.

Contents

1	Introduction	1
1.1	Thesis aims and objectives	2
1.2	Thesis structure	3
2	Literature Review	4
2.1	Single Screw Extrusion Control Models	4
2.1.1	Fuzzy Control	5
2.1.2	Soft Sensor approach	8
2.2	Melt Quality Control	9
2.2.1	Melt Temperature Control	9
2.2.2	Melt Pressure Control	11
2.2.3	Melt Viscosity Control	12
2.3	Other Findings	13
2.4	Previous work of Modeling in Single Screw Extrusion	13
3	Overview for Injection Molding Process	16
3.1	Screw Design	16
3.1.1	Sections of the screw and major functions	16
3.1.2	L/D Ratio	17
3.1.3	Screw Geometries	17
3.2	Review of Melt Temperature in Polymer Processing	19
3.2.1	Theoretical model of continuous melting	19
3.2.2	Experimental investigation on the effects of process settings on melt flow homogeneity	20
3.2.3	Experimental investigation on the measure of the pressure profile across the channel	21
3.2.4	Temperature measurement methods for single screw extrusion	22
3.2.4.1	Thermocouple mesh devices	22
3.2.4.2	Infrared Thermometer	22
3.2.4.3	Fiber Optical Pressure Sensor	24

3.3	Physical and Rheological properties of Polyethylene	26
3.3.1	Drying of PET Resin	28
3.3.2	Cross-WLF viscosity model	29
3.3.3	Polymer Melt Rheology	30
3.3.4	Polymer Melt Flow Rate	31
3.3.5	Polymer Melt Thermal Conductivity	32
4	Experimental Measurements of Extrusion Processes	33
4.1	Betol BC-60 Extruder	33
4.1.1	Material	33
4.1.2	Experimental equipment	33
4.1.2.1	Large scale single screw extruder	33
4.1.2.2	Screw geometry used in the large scale single screw extruder	35
4.1.2.3	Operating conditions used in the large scale single screw extruder	35
4.1.2.4	Monitoring techniques used in the large scale single screw extruder	36
4.1.3	Experimental Results	37
4.2	Husky IMS Injection Machine	37
4.2.1	Material	38
4.2.2	Experimental equipment	38
4.2.2.1	Monitoring techniques used in Husky IMS Injection Machine	38
4.2.2.2	Screw geometry used in Husky IMS Injection Machine	39
4.2.2.3	Operating conditions used in Husky IMS Injection Machine	40
4.2.3	Experimental Results	41
5	Basics for Regression Models	43
5.1	Introduction	43
5.2	Linear Least Squares Regression	44
5.3	Multiple Linear Regression	44
5.4	Regression Diagnostics	45
5.5	Measuring Performance in Regression Models	46
5.6	Model Evaluation	47
5.7	Analysis of Variance (ANOVA)	48
5.8	Principal Component Analysis (PCA)	49

5.9	Comparison of ANOVA and Regression	50
5.10	SPSS Program	51
5.11	The basics of Neural Network (NN)	52
5.12	Nonlinear Regression using ANFIS	53
6	Proposed Mathematical Modeling of the Die Melt Temperature Profile	55
6.1	Experimental Inputs for the Models creation (Missing Data filling)	55
6.2	Die Melt Temperature Profile Models	58
6.2.1	Arrhenius Model based on Linear Least Squares Regression	58
6.2.2	Model based on Multiple Linear Regression	60
7	Mathematical Modeling of the Single Screw Extruder Profile using ANFIS and comparing with other Mathematical Models	70
7.1	Experimental Inputs for the Models Creation	70
7.2	Statistical Verification of the Models	73
7.3	Die Melt Temperature Profile Modeling and Verification	74
7.3.1	Arrhenius Model based on Linear Least Squares Regression and Verification	74
7.3.2	ANFIS Verification Results	77
7.3.3	Comparison of Arrhenius and ANFIS model	79
7.4	Screw Speed Modeling and Verification	81
7.4.1	Arrhenius Model based on Linear Least Squares Regression and Verification	81
7.4.2	ANFIS Verification Results	83
7.4.3	Comparison of Arrhenius and ANFIS model	85
7.5	Final Single Screw Extruder Profile model	86
8	Conclusions and Future Work	87
8.1	Conclusions	87
8.2	Future Work	88
	References	89
	Appendix A	92
A.1	HDPE - B4020N1343	93
A.2	PET	94

Chapter 1

Introduction

Consumption of polymeric materials has greatly increased over the past few decades due to their use in diverse industrial sectors. Plastics are in high demand in the packaging, construction, automotive, electrical and electronics industries, in addition to many other diverse applications.

The extruder is arguably the single most important piece of polymer processing machinery. The injection molding process requires the use of an injection molding machine, raw plastic material, and a mold. Figure 1.1 depicts a typical single screw injection molding machine and its basic components. The plastic is fed through the hopper into the injection unit and melted by a combination of conduction through heating elements around the barrel and heat of dissipation through friction between the pellets and the screw. The final melt is then injected into the mold, where it cools and solidifies into the final part.

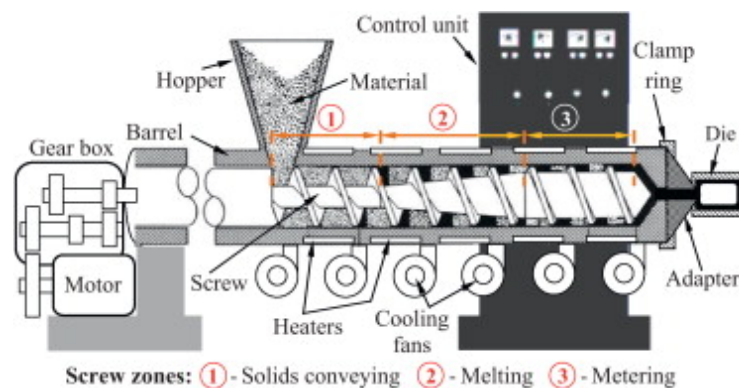


Figure 1.1: Basic components of a single screw extruder

Single screw extruders are controlled by setting barrel and die temperatures and screw rotation speed. The quality of extruded polymer is highly dependent upon the homogeneity of the molten polymer being fed into the die, which should ideally be supplied at a constant pressure, temperature and throughput.

Melt temperature is important for achieving a successful extrusion process as it has a significant impact on product quality. Variations in melt temperature that occur when the extruder is operated at high throughputs have been reported to be associated with melting instabilities. Screw design has been found to have a direct effect on melt homogeneity and hence quality of the final product (Kelly, Brown, Howell, & Coates, 2008). Extrusion variables should be then tailored to suit the performance of each individual extruder screw and polymer being processed.

So, the extrusion process is highly nonlinear as the thermal homogeneity of the melt is considerably affected by the process settings and melt flow temperature is different at different radial locations of the die (Abeykoon, Kelly, Martin, & Li, 2013). It seems that only a few control techniques which make control decisions by observing the actual melt flow quality are available. Therefore, the development of new control strategies which consider the actual melt quality, perhaps incorporating industrially popular nonlinear techniques (such as A.I.) is highly valuable.

1.1 Thesis aims and objectives

The main aim of this work was to propose novel mathematical control techniques (incorporating nonlinear techniques) which make control decisions by observing the actual melt flow quality in an attempt to investigate the problem of existing models in achieving consistent product quality. The overall objectives of this research were to:

- Examine real-time temperature techniques (such as a thermocouple grid sensor and an infrared temperature sensor) and real-time pressure techniques (like a fiber optical pressure sensor) in order to provide quantification of the thermal homogeneity of the single screw extrusion process.
- Investigate the effects of process settings (barrel temperature and screw speed) on melt flow homogeneity.
- Examine the rheology effects and the thermal properties of different polymers (HDPE and PET).

- Analyze basic regression models and diagnostics that will help for the creation and validation of this thesis single screw extrusion models.

1.2 Thesis structure

This thesis is divided into seven chapters. The literature review of Single Screw Extrusion models and controller algorithms is presented in Chapter 2. The overview for injection molding process, including the description of screw design, the review of melt temperature and physical and rheological analysis of Polyethylene are given in Chapter 3.

As there were not experimental data available for the model creation and validation, I used two experimental results from some previous investigations, which are presented in detail in Chapter 4. Chapter 5 shows some basic statistics info which are used for the model creation. Experimental inputs for the model creation and the proposed mathematical models of the die melt temperature profile for the single screw extruder are given in Chapter 6. Mathematical Modeling of the Single Screw Extruder Profile using ANFIS and Arrhenius and the final Single Screw Extruder Profile model is shown in Chapter 7. Finally, overall conclusions are presented in Chapter 8, with recommendations for further work.

Chapter 2

Literature Review

2.1 Single Screw Extrusion Control Models

Polymer extrusion is usually a complex process, particularly due to the coupled nature of process parameters, and hence highly prone to fluctuations. Presently, most of the polymer processing extruders are equipped with proportional-integral-derivative (PID) controllers mainly for the control of the screw speed and barrel temperatures in their set limits.

PID control has some serious drawbacks, which are ([Deng et al., 2014](#)):

- The parameters of the PID controller require long time to adjust
- A PID controller lacks robustness. The tuned parameters are suitable for a specific working condition or particular material only. Either change can lead to a re-tuning process which is not suitable for industrial applications.
- Multi-output is difficult to tackle in a PID controller. Melt outputs are correlated with each other, thus a multi-output controller is required to tackle them simultaneously, but the extension of a traditional single-input single-output PID algorithm to a multi-output system is difficult.

It seems that only both of these controllers are commonly used as the major aids of process control to achieve the required melt quality. Although, the quality of the melt output (i.e., a thermally homogeneous melt output which is constant in quantity and quality over the time) is the key variable in polymer extrusion, only a few control techniques are available which make control decisions by observing the actual melt flow quality. Some papers presented new control strategies which consider the actual melt quality allowing identification and control of process disturbances.

2.1.1 Fuzzy Control

Fuzzy control is an expert system which uses a rule-based decision making scheme. It is based on traditional boolean logic, but allows partial membership in a set. The process of fuzzy control is illustrated in Fig. 2.1

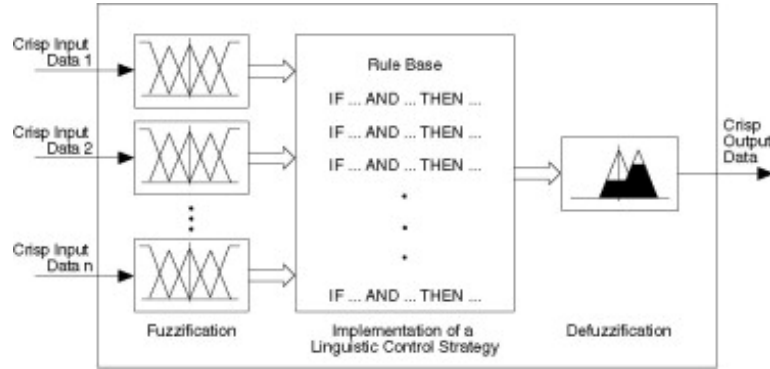


Figure 2.1: The process of fuzzy logic control
(Deng et al., 2014)

So, a typical fuzzy logic controller consists of three components:

- **Fuzzification:** input values are associated with linguistic variables through membership functions.
- **Rule design:** this describes the relationship between input and output linguistic variables.
- **Defuzzification:** the degree of membership of output linguistic variables within their linguistic terms are converted into crisp numerical values for controller output.

A fuzzy PID controller can be easily developed by taking the process error and error changes as crisp inputs. The membership function can be chosen to have a triangular, trapezoidal, sigmoid or Gaussian shape. The number of fuzzy rules depends on both the number of input linguistic variables and the number of linguistic terms associated with each variable. This can be simply calculated by:

$$N = p_1 \times p_2 \times \dots \times p_n \quad (2.1)$$

where p_i is the number of linguistic terms for the input linguistic variable i . Therefore, the number of fuzzy rules is very sensitive to the input variables.

Fuzzy controller seems a great alternative of PID for polymer extrusion, as (Deng et al., 2014):

- The membership function in fuzzy control is easier to adjust and previous experiences can be incorporated.
- Fuzzy control is more robust to both internal and external conditions, due to the linguistic nature of fuzzy rules, which is independent of the process model.
- Fuzzy control can easily tackle multi-output by incorporating these correlations into the rule design.

Alternative controllers based on fuzzy logic have been recently developed, providing satisfactory accuracy in processes with different extruder machines, geometries and processing materials.

(Abeykoon, Li, McAfee, Martin, & Irwin, 2011) proposed a model-based fuzzy control framework to reduce the die melt temperature variance while achieving the desired average die melt temperature. The controller determines the average melt temperature based on a radial temperature profile of the die melt flow. As seen in Figure 2.2, they used five process inputs (i.e. screw speed and four barrel zone temperatures) as the manipulated variables. Two fuzzy logic controllers (named as FLC 1 and FLC 2) provide the required control commands (based on 30 knowledge-based linguistic if-then fuzzy rules) to these process inputs to reduce the die melt temperature variations across the melt flow while achieving desired average die melt temperature.

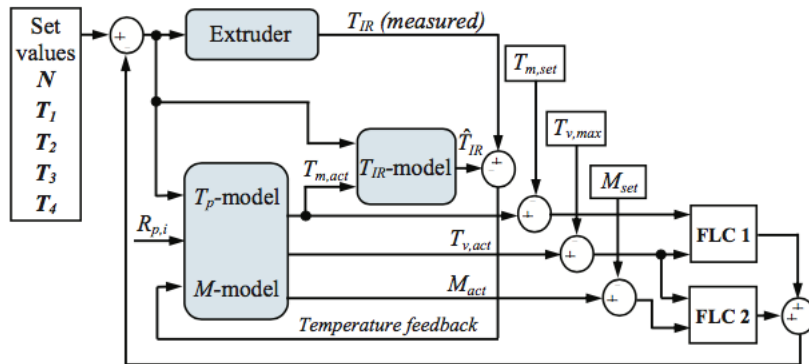


Figure 2.2: The purposed controller structure (Abeykoon, Li, McAfee, Martin, & Irwin, 2011)

As for the models used, a specially developed nonlinear polynomial dynamic model (T_p -model) is used to predict the melt temperature profile, a IR temperature prediction model (T_{IR} -model) is used to predict the melt temperature at each radial position across the die and a nonlinear model (M-model) was developed to predict the mass throughput as a function of process inputs. This model-based fuzzy control framework confirmed its efficacy.

(Deng et al., 2014) developed a fuzzy logic controller for the single screw extruder to maintain the melt pressure and melt temperature at desired levels. Melt viscosity is not included into the fuzzy control system, as it was difficult to measure due to lack of sensors. The fuzzy controller has four inputs: pressure error, change rate of pressure error, temperature error and the change rate of temperature error. The fuzzy controller outputs are adjusted values for screw speed and barrel heating temperature.

Inputs and outputs of the fuzzy system (E_p denotes the melt pressure error, ΔE_p is the change of pressure error, E_T and ΔE_T are melt temperature error and the change of such error, respectively, ΔN and ΔT_b represent change of screw speed and change of barrel heating temperature, respectively. Meanwhile, "I" is short for "Input", "O" is short for "Output", "neg" is short for "negative", and "pos" is short for "positive").

Variables	I/O	Linguistic terms
E_p	I	High neg, Medium neg, Central, Medium pos, High pos
ΔE_p	I	Fast neg, Slow neg, Zero, Slow pos, Fast pos
E_T	I	High neg, Medium neg, Central, Medium pos, High pos
ΔE_T	I	Fast neg, Slow neg, Zero, Slow pos, Fast pos
ΔN	O	High neg, Medium neg, Low neg Central, Low pos, Medium pos, High pos
ΔT_b	O	High neg, Medium neg, Low neg Central, Low pos, Medium pos, High pos

As seen on the Table above, each of the four inputs is associated with 5 linguistic terms, so total number of 625 rules are required for this control system design but for ease of implementation, 156 rules are used at last.

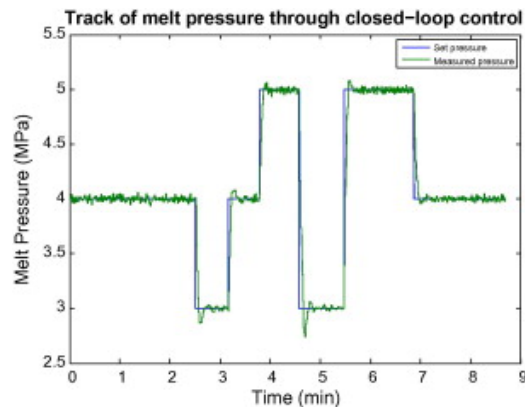


Figure 2.3: Pressure variation under fuzzy control

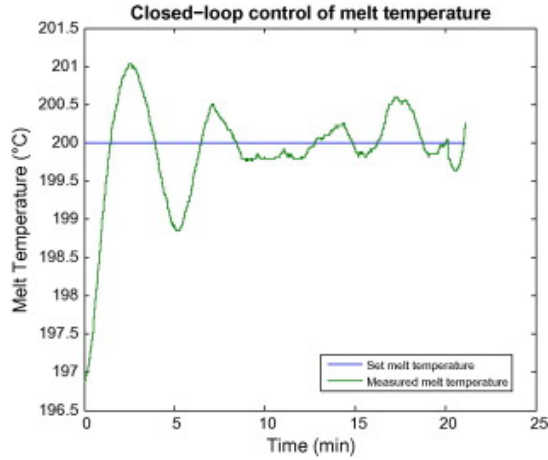


Figure 2.4: Temperature variation under fuzzy control

Figure 2.3 and 2.4 show the experimental results of pressure and temperature variation under fuzzy control (for temperature setting profile: 175-185-190-190-190-190-190 °C and the screw speed was automatically adjusted in the range of 5-60 rpm). For the pressure variation, it is observed that under fuzzy control it can be significantly reduced to ± 0.03 MPa, while for the melt temperature variation, after a settling time of nearly 6 min the variations become smaller than 0.5 °C.

It is shown that knowledge-based fuzzy rules provide good control capabilities to maintain the melt temperature homogeneity within desired limits by manipulating screw speed and barrel set temperatures in parallel. So this may offer a new method to operate extruders at high screw speeds whilst achieving both high energy and thermal efficiencies.

2.1.2 Soft Sensor approach

The principle of the soft sensor is based on a feedback observer mechanism, as shown in Figure 2.5.

For the single screw extrusion, melt viscosity is largely recognized as one of the most relevant indicators of melt quality. However, on-line viscosity measurement to a required standard has proved difficult to achieve. Soft Sensor approach proposed by (Liu, Li, McAfee, Nguyen, & McNally, 2012) solves this problem as seen in Figure 2.6. A viscosity model was identified based on the process inputs, such as barrel temperatures and screw speed, to infer the melted viscosity. The estimated melt viscosity, together with the screw speed, is then used as input variables for the pressure model to predict the barrel pressure. Finally, the predicted barrel pressure is compared with

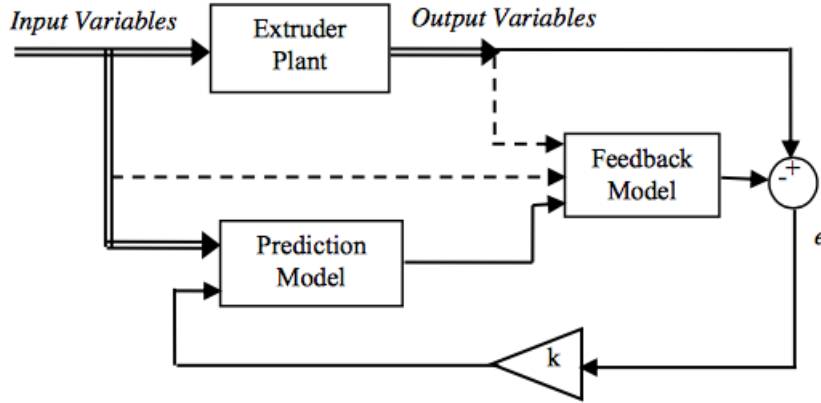


Figure 2.5: Schematic of the Soft-Sensor process
(Li & Martin, 2010)

the actual measured value, and the generated error used as a feedback signal to correct the estimated viscosity.

This novel feedback structure enables the online adaptability of the viscosity model in response to modeling errors and disturbances, hence producing reliable viscosity estimate.

2.2 Melt Quality Control

Many published papers studied single screw extrusion control and the effects of the quality the extrusion has on different polymers. Melt quality control approaches are based on temperature, pressure and viscosity which are the three main indicators of the melt quality.

2.2.1 Melt Temperature Control

(Sanjabi, 2010) investigated the effect of screw rotating speed on the melt temperature change in 3 different situations.

- **HDPE WITH GENERAL PURPOSE SCREW** A HDPE resin with MFI of 2g/10min and a general purpose screw (GP) were utilized in this situation. The experimental results show that the melt temperature increases by increasing the screw speed, regardless of the barrel heat setting temperature, due to the increased heat of dissipation.

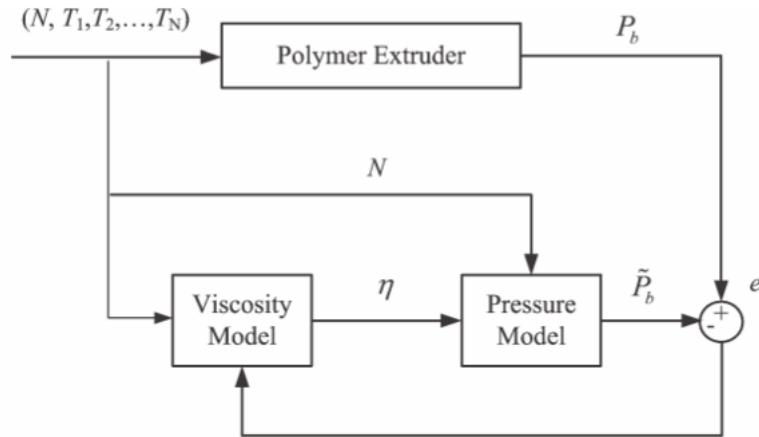


Figure 2.6: Soft-Sensor with a feedback structure for Single Screw Extrusion (Liu et al., 2012)

- **HDPE WITH BARRIER SCREW** The same HDPE resin as above was used here, but the screw type changed to a Barrier screw which is used widely for high-output, high-quality extrusion.

The experimental results show that the melt temperature depends on the screw speed, but compared to the GP screw, the melt temperature here is slightly higher due to the geometry of Barrier screw and the increase of melt temperature is more gradual.

- **PET WITH PET SCREW** A PET resin with intrinsic viscosity (IV) of 0.83 dl/g and a PET screw were utilized in this situation. The main difference with the HDPE resin situations is that here the initial temperature at the entry of the injection unit is already at a higher level due to the need of the PET to be dehumidified before processing. Even in this situation the conclusion was once again that increasing the barrel heat alone is not the lone source of providing heat to the melt and has less impact than screw speed.

In general, after these 3 different situations it was found out that the majority of heat required for melting is supplied by the heat dissipation due to friction between the screw and resin. In other words, the majority of the melt temperature rise comes from the screw speed. It was also found out that the geometry of the screw will greatly impact the final melt quality at the screw end and can generate either a homogeneous or inhomogeneous melt.

(Abeykoon et al., 2013) used in their experiment a HDPE resin with MFI

of 0.16g/10min and a general purpose screw. The results showed that the screw speed is the most significant process parameter affecting the level of melt temperature and thermal homogeneity across the melt flow. They also claim that the melt flow temperature is different at different radial locations of the die.

(Geissler, 2006) investigated the flow characteristics of PET resin at different temperatures. He found for this product that for increasing shear rates, the influence of barrel temperature in the polymer melt temperature decreases. In other words this means that for higher shear rates melt temperature (and therefore, melt quality) depends on the screw speed and not from the barrel temperature settings. On the other hand, for low shear rates the flow characteristics of polymer melts can vary at different processing temperatures.

2.2.2 Melt Pressure Control

(Sanjabi, 2010) investigated melt pressure during screw recovery in the 3 different situations mentioned in 2.1. It was found that Barrier screws build up initial pressure faster than general purpose (GP) screws, but for the remainder of the screw length the melt pressure is more steadily increasing, offering stability of the process and reduction of wear and tear.

In general, those three experiments showed that any increase in melt temperature will decrease the melt pressure during recovery. It was also found out that under constant barrel temperature the melt pressure is normally proportional to screw speed, that is, as the screw rotational speed increases, the melt pressure along the length of the extruder increases too.

(Deng et al., 2014) showed the importance of melt pressure control, as they claim that it has been shown as a cost-effective alternative to mechanical volumetric pumps, reducing by this way the energy consumption. In this paper, a LDPE (low density polyethylene) resin and a general purpose (GP) screw were used for the experiments.

The results showed that the melt pressure is normally proportional to screw speed and change of screw speed will naturally introduce an over-shoot in the melt pressure. So any increase in melt temperature will decrease the melt pressure. They also claim that compared to melt temperature, pressure is easier to control in the extrusion process due to its quick response to a change in screw speed.

2.2.3 Melt Viscosity Control

Viscosity according to many studies, is considered a better indicator of melt quality, compared to melt pressure and temperature. The viscosity of a polymer melt can generally be considered as a function of shear rate, temperature and pressure.

(Deng et al., 2014) describe viscosity as the resistance of material to flow, and is derived from the shear stress and shear rate of the flow, as shown in this equation:

$$\eta = \frac{\tau}{\dot{\gamma}}$$

where η represents the viscosity, τ is the shear stress and $\dot{\gamma}$ denotes the shear rate. Shear stress is determined by the pressure drop in a slit die, while the shear rate is proportional to the volumetric flow rate through the die.

In extrusion, polymer melts are in a predominantly shear flow regime where the viscosity follows a power-law relationship. For shear stress in a slit die, viscosity can be calculated using:

$$\eta = \frac{\Delta P W H^2}{12 L Q} \frac{3\bar{n}}{2\bar{n} + 1}$$

where \bar{n} is the power law index under the operating conditions, ΔP denotes the pressure drop along the slit die, W and H are the slit width and height, L is the length between the two pressure points and Q represents the volumetric flow rate.

(Deng et al., 2014) after investigating viscosity in the experiment described in 2.2, found out that any increase in melt temperature will decrease the viscosity. They also claim that viscosity is probably the best quality indicator but also the most difficult one to control as it is not directly measurable. The in-line viscometers, a common method of making viscosity measurements, are not industrially attractive due to their possible disruptions on the steadiness and rate of the melt flow and their high cost. Advanced control, incorporating soft-sensor approach is an alternate option, but it has accuracy issues. So, the authors propose for future work a soft-sensor approach, but with accuracy improvement leading to real-time monitoring of melt viscosity.

(Sanjabi, 2010) after doing the 3 experiments described in 2.1, found that the melt viscosity reduces with increasing the average temperature, but they

also found out that at some point during the melt temperature rise, which is normally above the suggested melting point of the polymer, increasing melt temperature further will not impact the viscosity significantly, because all polymer chains are now melted and the polymer has reached its minimum achievable viscosity.

(Geissler, 2006), as mentioned in 2.1, showed that for PET resin the influence of the temperature decreases for increasing shear rates. So, the viscosity is independent of temperature fluctuations at higher shear rates.

2.3 Other Findings

(Deng et al., 2014) found out that in addition to the control of melt temperature, the melt thermal homogeneity was also shown to be a key factor both for the product quality and for energy consumption. (Abeykoon et al., 2013) agree with that and also claim that the thermal homogeneity of the melt is considerably affected by the process settings.

(Rasid & Wood, 2003) found that the metering zone had the highest influence on the melt temperature. (Abeykoon et al., 2013) agree with that, as they say that the metering zone temperature is the most significant among the barrel zone temperatures. On the contrast, (Abeykoon, Li, McAfee, Martin, Niu, et al., 2011) say that the melting zone temperature is the most critical barrel zone temperature affecting the die melt temperature profile.

2.4 Previous work of Modeling in Single Screw Extrusion

The extrusion process is highly non-linear. Some static and dynamic nonlinear models have been developed to explore the effects of process settings and screw geometry on melt temperature development in single screw extrusion.

(Abeykoon, Li, McAfee, Martin, Niu, et al., 2011) presented a novel static nonlinear polynomial model to predict the die melt temperature profile from readily measured process parameters. The main aim was to model the effects of process settings on the shape of the die melt temperature profile. Six model inputs (ω_{sc} , R_p , T_1 , T_2 , T_3 , T_4) and one output ($T_{p,die}$ - melt temperature at a specified radial position of the die) were considered as showed in Figure 2.7 and it is obvious that this steady-state model predicts the melt temperature values of the each radial position assigned by the radial position input. (11 radial positions totally. R_p inputs: 0 mm, ± 3 mm, ± 5 mm, ± 8.5 mm, ± 15 mm and ± 19 mm).

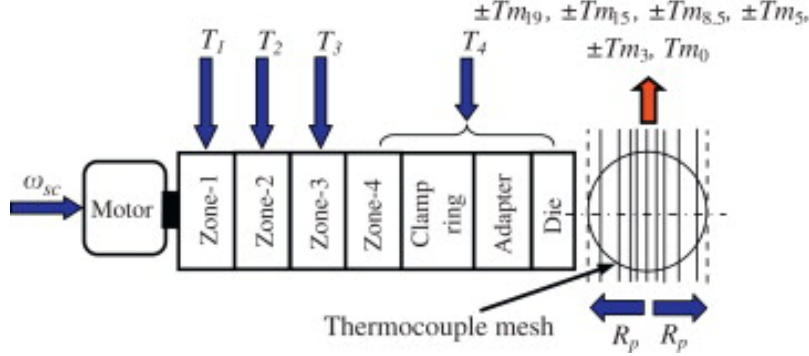


Figure 2.7: Extruder model with selected inputs and outputs

So, with constant screw speed and barrel set temperatures, the model estimates the melt temperature values of these 11 points individually by only changing the radial position input.

Finally, a 6th order model with 12 terms was selected for this nonlinear static melt temperature profile $T_{p,die}$ prediction model:

$$\begin{aligned}
T_{p,die} = & [1.256 \times T_2] && + [1.835 \times 10^{-03} \times R_p^2 \times T_4] \\
& + [5.717 \times 10^{-09} \times \omega_{sc}^4 \times R_p^2] + [0.581 \times \omega_{sc}] \\
& + [2.642 \times 10^{-07} \times \omega_{sc}^2 \times R_p^4] - [1.528 \times 10^{-05} \times \omega_{sc} \times R_p^4] \\
& - [1.275 \times 10^{-06} \times \omega_{sc}^3 \times R_p^2] + [2.057 \times 10^{-03} \times \omega_{sc} \times R_p^2] \\
& - [5.635 \times 10^{-13} \times \omega_{sc}^2 \times T_4^4] - [2.118 \times 10^{-03} \times R_p^2 \times T_3] \\
& + [1.469 \times 10^{-11} \times \omega_{sc}^5 \times T_4] - [2.859 \times 10^{-05} \times \omega_{sc}^2 \times T_1]
\end{aligned}$$

This model shows a good fit of 84.38% fit with the unseen data (with root mean square errors - RMSE = 2.89). Any differences found are mostly due to the dynamic behavior of the measured data whilst the developed model is a static model.

In a newer study from the same authors ([Abeykoon et al., 2013](#)) presented a novel **dynamic** polynomial model, with the same aim and same concept (inputs/outputs) as their previous work in general. This model aims to predict the melt temperature values of each radial position assigned by the radial position input, measured using a thermocouple mesh placed in-between the adapter and the die (Figure 3.5), with 15 radial position inputs in total this time (R_p inputs: 0 mm, ± 3 mm, ± 4.5 mm, ± 8.8 mm, ± 11 mm, ± 14.7 mm, ± 16.5 mm and ± 19 mm).

So, with constant screw speed and barrel set temperatures, the model estimates the melt temperature values of these 15 points individually by

only changing the radial position input.

With the use of a fast recursive algorithm (FRA) for a recursive solution and a backward model refinement procedure to eliminate non-significant terms, a 2nd order model with 14 terms was selected for this nonlinear dynamic melt temperature profile prediction model:

$$\begin{aligned}
\hat{T}_{m,j}(t) = & 1.6128 \times \hat{T}_{m,j}(t-1) - 0.0048 \times \hat{T}_{m,j}(t-1) \times R_{p,j} \\
& + 0.0071 \times R_{p,j} \times T_4(t-60) - 0.0870 \times \hat{T}_{m,j}(t-2) \\
& + 0.0018 \times \omega_{sc}(t-10) \times R_{p,j} + 0.0001 \times T_3(t-90)^2 \\
& - 0.0080 \times \hat{T}_{m,j}(t-1) \times T_1(t-150) - 0.4998 \times T_4(t-60) \\
& - 0.0045 \times \hat{T}_{m,j}(t-2) \times \omega_{sc}(t-10) + 0.2806 \times \omega_{sc}(t-10) \\
& + 0.0032 \times \hat{T}_{m,j}(t-1) \times \omega_{sc}(t-10) - 0.0200 \times R_{p,j}^2 \\
& + 0.0079 \times T_1(t-150) \times T_4(t-90) - 0.6378 \times R_{p,j}
\end{aligned}$$

This model shows a fit of 80.06% fit with the training data (with root mean square errors - RMSE = 2.62) and a 78.24% fit with the unseen data (RMSE=2.86)

Chapter 3

Overview for Injection Molding Process

3.1 Screw Design

The extruder screw is widely acknowledged as being the most important mechanical element of a single screw extruder. The design of the screw is of paramount importance for optimisation of the extrusion process and quality of the extruded polymer.

3.1.1 Sections of the screw and major functions

The major functions of a conventional extruder screw are achieved at different sections of the screw which may vary in length and configuration depending upon operation and polymer type being processed. In general, as shown in Figure 3.2 the three main functional/geometrical zones are:

1. Feeding zone (solids conveying)
2. Melting zone (or compression/plastication zone)
3. Metering zone (or pumping zone)

As can be seen in Figure 3.2, the screw shaft diameter increases gradually in the melting zone.

The **feeding zone** brings the feedstock into the extruder and moves the material along the screw. The polymer is then conveyed forward and compressed. This section is usually confined to the first few turns.

The **melting zone** comprises the major portion of the screw in which the polymer is gradually melted by simultaneous application of external heating from the barrel and internal viscous shear.

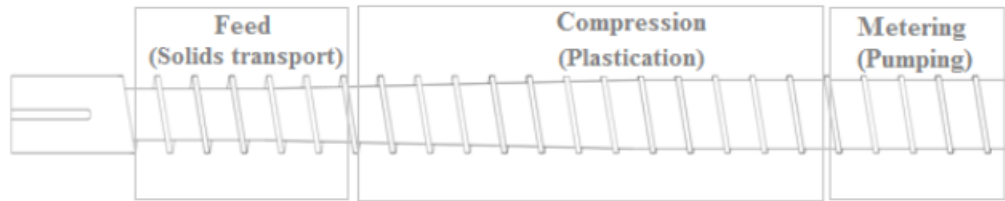


Figure 3.1: Sections of the extruder screw

The **metering zone** is usually confined to the last few turns on the screw where the uniformity of the melt is increased. In this section, the melt acquires the required pressure to flow through the section of the die.

3.1.2 L/D Ratio

Screw length is referenced often to its diameter as L/D ratio. The L/D ratio is the ratio of the length of the screw to its outside diameter. The ratio calculation is calculated by dividing the length of the screw by its nominal diameter. It is the most referenced term of the basic components of an extruder screw. The L/D ratio is a major factor in the effectiveness of the extruder and of the types of material that it can process.

Although several injection molding machine manufacturers now offer a choice of injection units, most injection screws use a 20:1 L/D ratio. (Reiloy, 2015)

3.1.3 Screw Geometries

Plenty of different extruder screws are available for different operating conditions. Three extruder screws, representative of those typically used in the polymer industry, are shown here:

1. Tapered Compression Screw (TA)
2. Stepped Compression Screw (ST)
3. Barrier Flighted Screw (BF)

Schematic representations of the screw designs are shown in Fig. 3.3.

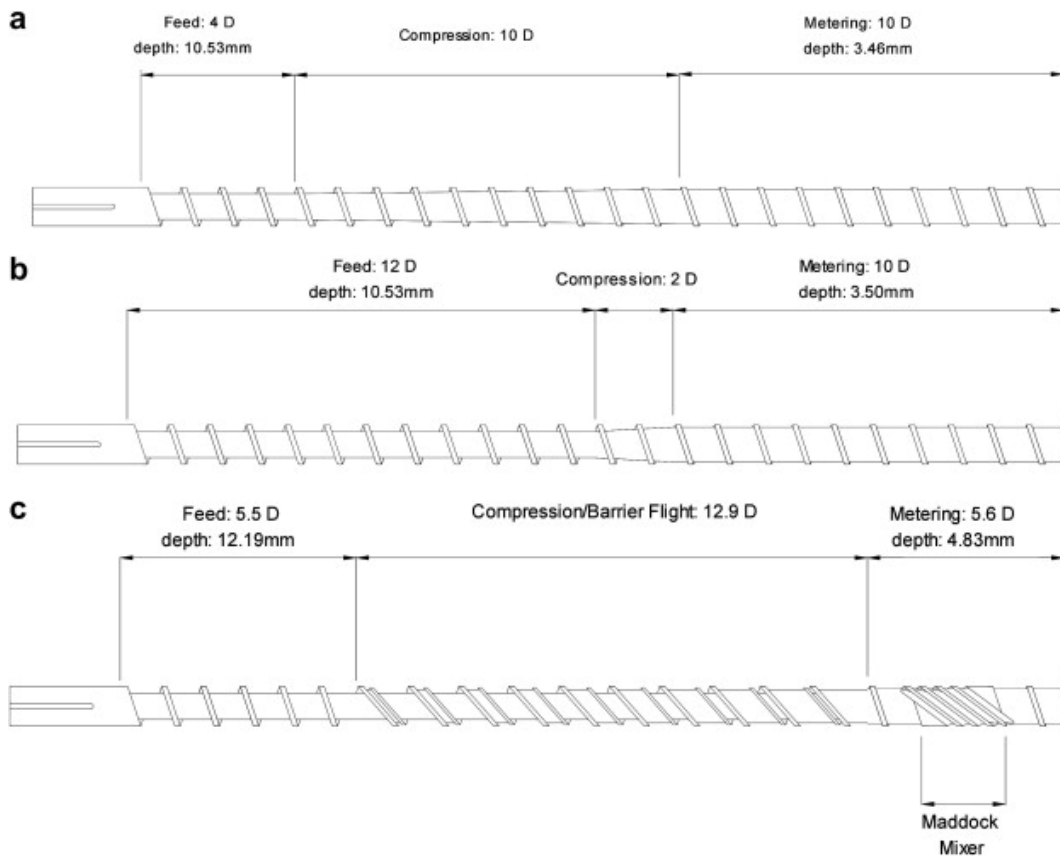


Figure 3.2: Extruder screw geometries (All screws are with a L/D ratio of 24:1) a) Single flighted, tapered compression. b) Single flighted, stepped compression, c) Barrier flighted with spiral mixer
(Vera-Sorroche et al., 2014)

Compared to the other 2 screw geometries (and every single flighted Conventional or General Purpose screw), barrier-type screws offer more homogeneous melting to facilitate uniform die flow, usually without the need for add-on mixing sections.

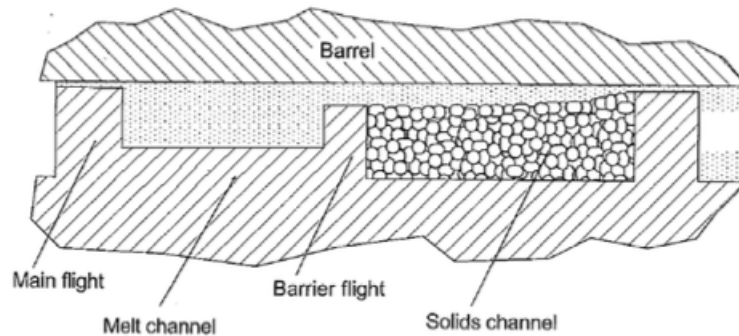


Figure 3.3: Cross section of a Barrier screw.
(Sanjabi, 2010)

As it can be seen in Figure 3.4, in Barrier screws the solid material is kept separate from the melt in the melting section. The main function of these screws is to separate the melted polymer from the solid bed and keep the solid bed from becoming unstable and prematurely breaking up. With a Barrier screw the rate of the melting is more gradual than the melting rate with a conventional/general purpose screw.

3.2 Review of Melt Temperature in Polymer Processing

3.2.1 Theoretical model of continuous melting

It is desirable that a single-screw extruder has the highest throughput with good quality polymer melt at the extrudate. For most polymers, however, the main factor which limits the throughput of an extruder is the melting rate of the polymer. If the melting rate in the extruder is not large enough, it may cause solid polymer fragments to be discharged from the extruder. Therefore, a good understanding of the melting behavior in the extruder is key for an optimum design and operation of a single-screw extruder.

For the evaluation and calculation of the melting behavior and the temperature profile over the screw length, the radial temperature profile inside the screw channel has to be evaluated.

During past five decades, numerous investigations have been performed on the topic of melting mechanism in plasticating extruders. Maddock (1959) was the first one to obtain a significant understanding of melting in a single-screw extruder. He observed that the first melt appears as a film of molten

polymer between the hot barrel and compacted solid pellets (solid bed). The polymer in the melt film is scraped by the active (pushing) flight of the screw to form a melt pool near the screw flight (Fig. 3.3). As the polymer in the melt pool increases, it exerts a considerable pressure on the solid bed causing it to deform continuously such that the width of the solid bed decreases along the channel, whereas the height of the solid bed remains at essentially the depth of the channel. The relative speed between the screw and the cylinder is called V_{rel} .

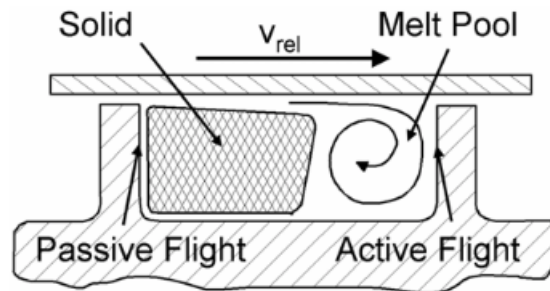


Figure 3.4: Melting model based on Maddock

3.2.2 Experimental investigation on the effects of process settings on melt flow homogeneity

In the extrusion process heat generation is achieved by barrel conduction and viscous heating by the mechanical work of the screw (which is dependent on screw speed, material and nature of the machine surfaces)

According to (Abeykoon, Li, McAfee, Martin, Niu, et al., 2011) melt flow homogeneity is highly dependent on screw speed (viscous heating). That's because increases in screw speed increase the **melt temperature** which affect directly melt flow homogeneity. Moreover, screw speed affect **material residence time** which is also a key factor in melt flow homogeneity. On the other hand, barrel temperature changes (barrel conduction) are not so significant on the melt flow homogeneity as the screw speed is.

Eventhough barrel temperature changes don't contribute so much in the homogeneity as the screw speed does, it is preferable for a better thermal homogeneity to control both screw speed and barrel set temperatures at optimum throughput and efficiency conditions. So a correlation between process settings and resulting melt flow homogeneity is necessary.

Some research work tried to study melt flow homogeneity based on melt temperature profile measurements. (Wood & Rasid, 2003) found that the me-

tering section barrel temperature had the major effect on melt temperature when compared to compression and feed barrel set temperatures. Another study by (Kelly et al., 2008) highlighted the effect of screw geometry on melt temperature profiles. They observed a strong effect of screw geometry on melt temperature as a result of the dependence of melting performance on extruder screw speed. cite (Abeykoon, McAfee, Li, Kelly, & Brown, 2010) found that if screw speed increases, the temperature variations increase too. They also found that barrel temperature changes influence the profile to a lesser extent than screw speed does. (Bur & Roth, 2004) found that the temperature profile is dependent upon screw speed, screw geometry and material.

3.2.3 Experimental investigation on the measure of the pressure profile across the channel

Some investigations about the measure of the pressure profile across the channel were made (Anger, Potente, Schöppner, Enns, et al., 2009) and shown that the peak of the pressure profile is in front of the active flight and decreases over the flight, with the minimum pressure to be at the passive flight. Inside the screw channel the pressure level increases continuously from the passive to the active flight, as shown in Figure 3.4

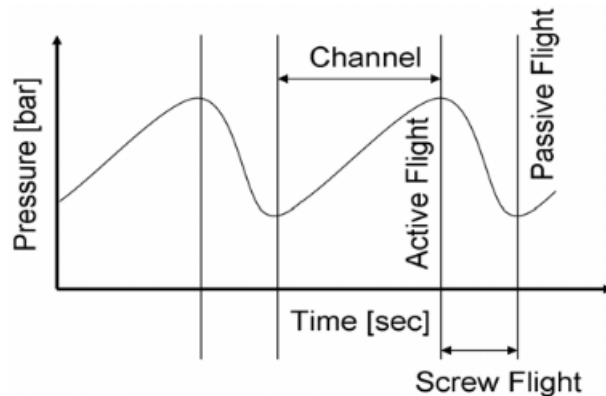


Figure 3.5: Melting model based on Maddock

3.2.4 Temperature measurement methods for single screw extrusion

3.2.4.1 Thermocouple mesh devices

Thermocouples meshes or grids were developed in an attempt to provide 2D profiles of temperature of a flowing melt.

Previous study by (Kelly et al., 2008) had confirmed that the die melt temperature measurements are symmetrical across the thermocouple mesh centreline when averaged over significantly long periods of time. Therefore, (Abeykoon, Li, McAfee, Martin, Niu, et al., 2011) placed asymmetrically across the die melt flow (between the adapter and the die, Figure 3.5) five thermocouple junctions (i.e. with a one negative and five positive thermocouple wires) along the diameter of the mesh as shown in Figure 3.6. This asymmetric placement of wires gave the opportunity to increase the measurement resolution across the melt flow, by mirroring these five melt temperature points over the die centreline to obtain the complete die melt temperature profile.

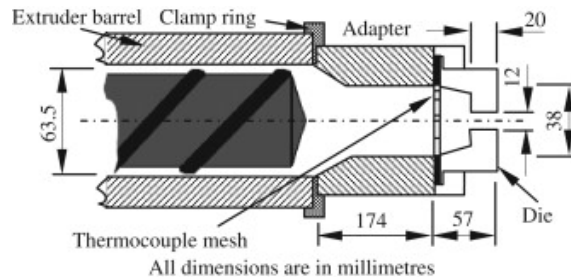


Figure 3.6: Extruder die, adapter and thermocouple mesh (Abeykoon, Li, McAfee, Martin, Niu, et al., 2011)

Thermocouple meshes enabled examination of the thermal dynamics of the extrusion process collecting information relating to short-term melt temperature changes. However, these devices cannot be used to measure temperature inside the extruder barrel.

3.2.4.2 Infrared Thermometer

Infrared sensors offer a non-intrusive method of temperature measurement. Infrared thermometers can be used to measure the temperature of a polymer by detecting the thermal radiation of a molten polymer (source) via a glass or sapphire window along optical fibers and consequently transformation of the received infrared radiation into an electrical signal (Figure 3.7)

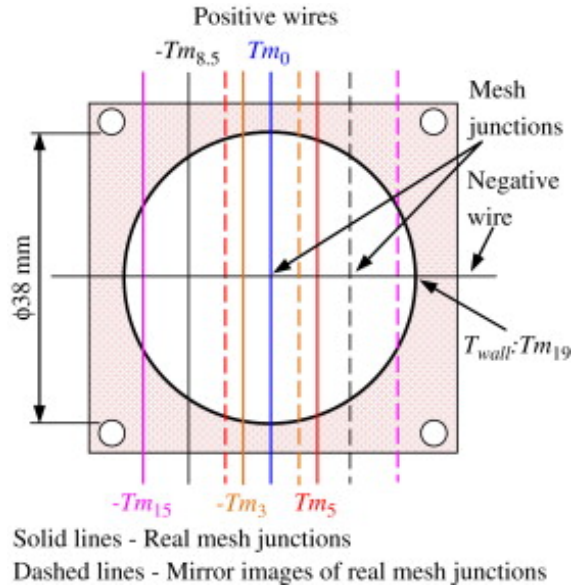


Figure 3.7: Arrangement of the thermocouple mesh (Abeykoon, Li, McAfee, Martin, Niu, et al., 2011)

According to (Anger et al., 2009) transmission of the infrared melt radiation to an infrared detector has response time about 10 milliseconds. They also mention that the IR detector is sensitive to the power of the radiation passing the sapphire window, generating an electrical voltage signal proportional to the incoming radiation power.

The non-invasive nature and rapid dynamic response of infrared thermometry (1000 times faster than best conventional thermometers) make it particularly suitable for extrusion applications and it has been used to provide temperature measurements of polymer melt inside the screw channel. In addition, the sensor itself is sensitive to changes in surface emissivity which enables measurements of residence time distributions.

Novel IR thermometers by (Anger et al., 2009) with an axially shiftable measuring tip have been used to measure radial temperatures profiles inside the screw channel of a single screw extruder using a tapered compression screw with a shearing and mixing zone. Several points of measurement along the axis with the barrel were used to build the temperature profile over the length of the screw (Figure 3.8). This thermometer combines a variable physical penetration depth with a fast responding IR temperature measuring technique.

Specifically, this infrared thermometer is equipped with two small thermocouple thermometers with fast response time (10 sec) at the front end of

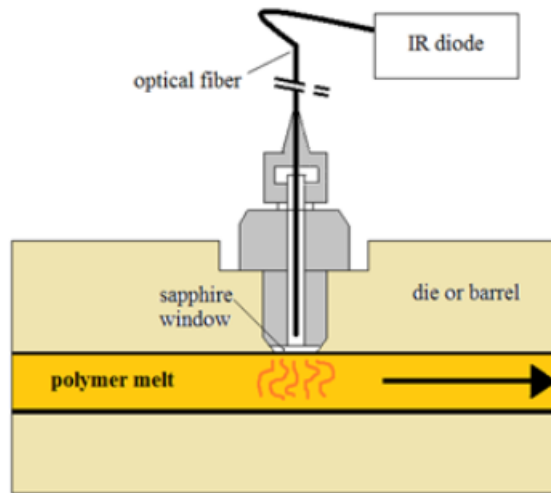


Figure 3.8: An infrared melt temperature sensor

the probe, to give absolute temperature readings from the melt [TIP(3)] and for calibration purposes [SENSOR-BODY(2)] of the IR-thermometer. The IR-measuring tip can be shifted precisely up to 5mm radial into the melt, as the Figure 3.8 shows, so as to measure the temperature profile from the barrel wall up to 5mm down to the ground of the screw channel. The other measuring points shown in Figure 3.8 are [IR(1)] which is the sapphire window for the IR-radiation input, [SEALING(5)] which is the thermocouple that detects the temperature of the barrel in the sealing area and [FRONT(4)] which is the thermocouple that detects the internal surface temperature at the interface of the barrel and the melt.

However, the precise area or volume of melt measured by infrared sensors is unclear and known to be material dependent and therefore, the operating distances of these devices are limited (Bur & Roth, 2004). When located in the extruder die adaptor, infrared sensors have been shown to detect temperature fluctuations related to melting instabilities but these were small in magnitude due the large diameter (38 mm) of the region of measurement compared to the relatively small effective penetration of the sensor (Kelly et al., 2008)

3.2.4.3 Fiber Optical Pressure Sensor

Fiber optical pressure sensors were developed in an attempt to provide the measurement of the pressure profile in the feeding across the screw channel without being destroyed. According to (Anger et al., 2009) the pressure

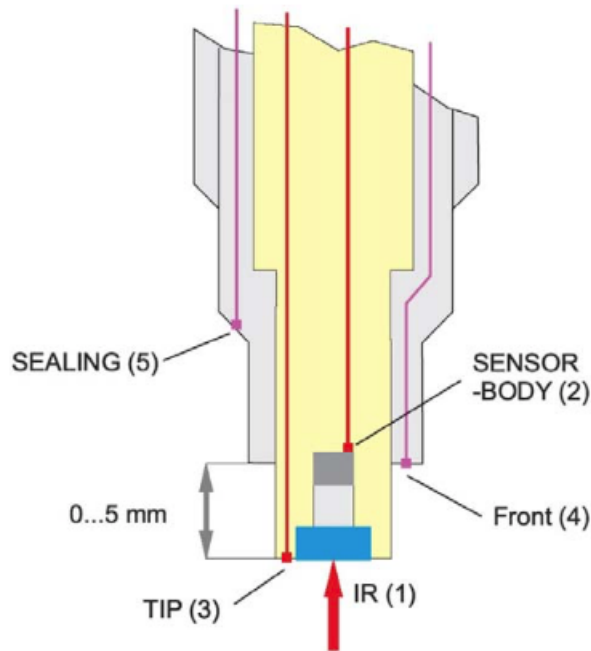


Figure 3.9: Measuring points being integrated in the infrared thermometer (Anger et al., 2009)

sensor could be used until 1000°C and the membrane is nearly indestructible, making it wear resistant and shear off strong. Also, they claim that the response time is very fast and it can be used for high dynamic processes.

Fiber-optical pressure sensors rely on the principle of changing the properties of light that propagate in the fiber due to the effect of the pressure parameter.

In general, the fiber-optical sensor is the light modulator, i.e., the entity that causes a light property (optical power) to change under the influence of a certain physical quantity (pressure). Thus a physical quantity can change the physical properties of the sensing element, which, in turn, leads to a change in the light properties.

A fiber-optical sensor system has four basic components: the light source (LED), the optical fiber (OF), the sensor element and the light detector (PD 1, PD 2). The light source provides the electromagnetic radiation whose energy is transmitted through the OF to the detector PD2 across the X-branching point as well as to the sensor head, in general, under the principle of total internal reflection, and by this way the power of the coupled light is exactly measured.

As it can be seen in Figure 3.9, in the sensor head in the back of the mem-

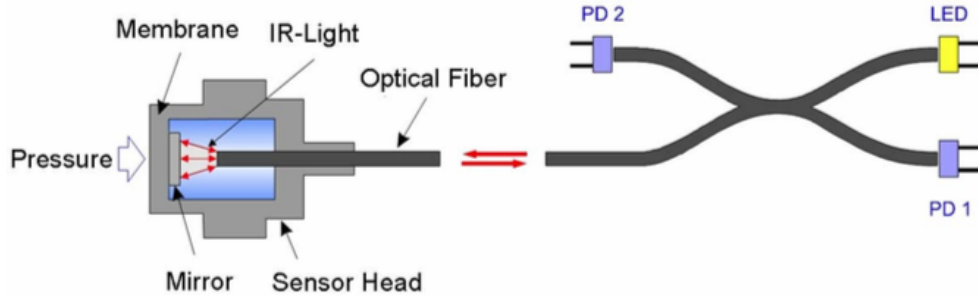


Figure 3.10: Measuring points being integrated in fiber optical pressure sensor

(Anger et al., 2009)

brane is placed a mirror which is a platinum reflector movable mirror. The distance between the mirror and the surface of the glass fibre varies according to the pressure acting on the membrane (by several micrometers under full pressure action (Anger et al., 2009)). More or less back-reflected light goes into the same fiber and is guided back to an amplifier. The amplifier is an optoelectronic detection device which compares the light intensity coming from the sensor head to the one transmitted. By making this comparison, the pressure at the sensor head is measured. Through the X-branching point, the light is conveyed to the detector PD1 and converted from light signal to electric current. So, the back-reflected intensity decreases, when the distance between the mirror and the PD1 increases (lower pressure on the membrane) and the back-reflected intensity increases, when the distance between the mirror and the PD1 decreases (higher pressure on the membrane).

Based on the above, this measuring system is a non-contact working and high-definition faser-optical measuring system. It can be used for high dynamic processes and is very wear-resistant, even with abrasive materials (like polymer in our case)

3.3 Physical and Rheological properties of Polyethylene

Two different polymers, High Density Polyethylene (**HDPE**) and Polyethylene Terephtalate (**PET**) are among the most widely used engineering plastics in the polymer industry. Some of the properties of the resins utilized are presented in Figure 3.10.

High Density Polyethylene (HDPE) was supplied by BP SOLVAY and is a high-density polyethylene copolymer (Eltex B4020N1343) suitable for use in injection and compression moulding applications, where high environmental stress cracking resistance is required (particularly intended for the injection moulding and compression moulding of screw caps for the packaging of beverages)

Polyethylene Terephthalate (PET 1101) was supplied by INVISTA CANADA and is a copolymer packaging resin. It is used successfully in carbonated soft drink bottles and other applications such as water bottles, food containers, and packaging for household goods.

Physical properties	PET	HDPE	Units
IV	0.83	-	dl/g
MFI	-	2.0	g/10min
Density	1.40	0.94	g/cm ³
Melting Point	245	138	°C
Melt Density	1.2	0.8	g/cm ³
Specific Heat Capacity	1.94	2.25	J/g°C
Heat of Fusion	65.5	45.0	J/g

Figure 3.11: Some physical and rheological properties of the solid HDPE and PET grades provided by the resin suppliers
(Sanjabi, 2010)

IV (intrinsic viscosity) is a measure of the polymers molecular weight and therefore reflects the material's melting point, crystallinity and tensile strength. The IV is used as part of the specification to select the right grade of PET for a particular application (AZoMaterials, 2009). PET has a unique ability to dramatically increase the viscosity of the liquid it is dissolved in, even at very low concentrations. IV is a quantitative assessment of this ability. PET 1101, as can be seen in Figure 3.10 has a nominal intrinsic viscosity of 0.83 dl/g.

The MFI (melt flow index) is a measure of the ease of flow of the melt of a thermoplastic polymer. The Melt Flow Index Formula is:

$$\text{MFI (In Grams)} = \text{Weight of Melted samples in 10 minutes}$$

HDPE Eltex B4020N1343 has a melt flow index of 2.0 g/10min.

Rheological parameters of the polymers are related to the melt density, specific heat capacity, heat of fusion, and melting temperature.

Melt density is the density of the material in the melted state. It is an important parameter in many aspects of rheology and in the plastic-technology industry. The melt density for a particular temperature and pressure environment is often required for different design considerations, such as in the design of an extruder screw, or in the design of a runner system of an injection mould, etc. (Liang, Li, & Tjong, 1999)

Specific Heat Capacity is the amount of heat required to change the temperature of one unit mass of a material by one degree.

Heat of Fusion is the amount of heat required to convert a solid at its melting point into a liquid without an increase in temperature.

More information of relevant properties of these polymers can be found in Appendix A.

3.3.1 Drying of PET Resin

Unlike the other major packaging resins (e.g., polyolefins, polystyrene, and PVC), PET is produced by a condensation reaction. Various starting materials are used and reacted in a series of steps to produce PET. This reaction, which also produces water, is reversible. Therefore, when undried PET is melted, the resin and water chemically react. Hydrolysis occurs and key mechanical properties of the PET are reduced. This hydrolysis reaction also changes PET melt viscosity and crystallization rate, making it very difficult to process into a quality end-product.

To avoid PET hydrolysis (and end-product quality decrease), PET must be thoroughly dry just prior to melt processing. Most PET drying is done in dehumidifying hoppers using hot air at a very low dew point. The dehumidified air passes through a bed of PET to extract moisture from the resin. A desiccant material, such as silica, absorbs moisture from the circulating air. PET must be dried to <30 parts per million and maintained at this moisture level to minimize hydrolysis during melt processing. A dry resin will help control the Intrinsic Viscosity (IV) loss, which should be less than 0.02 dl/g (which is the acceptable industry standard for the drop in the IV of the PET resin after the drying process). Controlling IV loss is critical to maintaining impact strength, stiffness, chemical resistance, melt viscosity, and other key properties of the starting material.

The PET should be dried at 170-180°C, so as a result, the initial PET resin temperature in the simulation tool is usually between 170 to 180°C compared to HDPE, which is at room temperature.

3.3.2 Cross-WLF viscosity model

According to (Sanjabi, 2010) the viscosity of the polymer melt is not constant and depends on temperature of the melt as well as the zero shear rates (and consequently the velocity fields of the polymer melt)

Several models are presented to study the shear thinning behavior of polymer melts. The Cross-WLF model is more appropriate for injection molding simulations as temperature and shear rate effects are better represented.

The following equations illustrate the Cross-WLF viscosity model:

$$\eta = \frac{\eta_0}{1 + \left(\frac{\eta_0 \dot{\gamma}}{\tau^*}\right)^{1-n}}$$

where:

- η is the melt viscosity (Pa s)
- η_0 is the zero shear viscosity or the 'Newtonian limit' in which the viscosity approaches a constant at very low shear rates
- $\dot{\gamma}$ is the shear rate (1/s)
- τ^* is the shear thinning transition (Pa)
- n is the power law index in the high shear rate regime

$$\eta_0 = D_1 \exp\left[-\frac{A_1(T - T^*)}{A_2 + (T - T^*)}\right]$$

where:

- T is the temperature (K)
- T^* is the pressure dependent constant temperature (K) which is equal to $D_2 + D_3 P$ where D_2 and D_3 are plastic material constants
- $A_2 = A_3 + D_3 p$
- p is the pressure (Pa)

The zero shear viscosity (η_0) can be represented by the WLF form as follows:

where T_g is the glass transition temperature of the material and n , τ , D_1 , D_2 , D_3 , A_1 , A_2 are model constants.

- $T \geq T_g$, $\eta_0(T, p) = D_1 e^{-A_1(t-T_g) / (A_2+t-T_g)}$
- $T < T_g$, $\eta_0(T, p) = \infty$

3.3.3 Polymer Melt Rheology

In single screw extrusion, melt viscosity is clearly affected by shear and changes nonlinearly with shear rate. The viscosity of the polymer generally exhibits non-Newtonian pseudoplastic flow behaviour, as shown in Figure 3.11

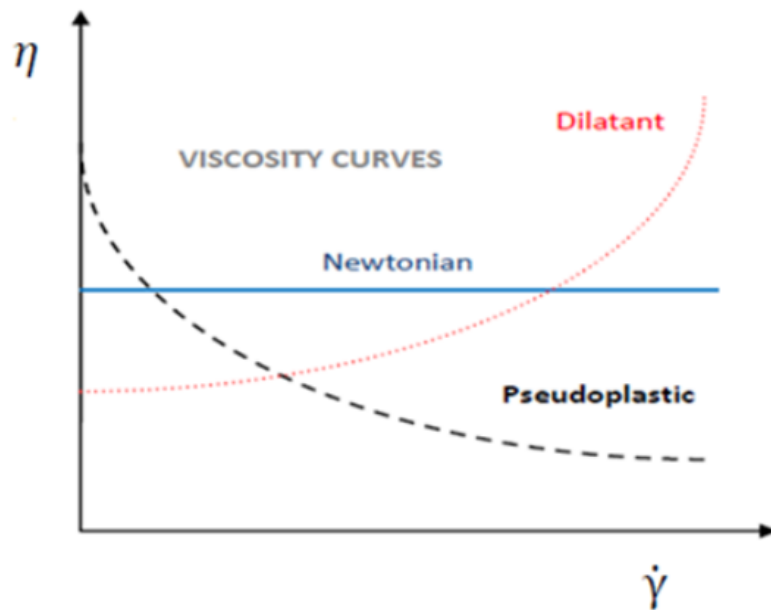


Figure 3.12: Non-newtonian pseudoplastic flow behaviour

Temperature, pressure, shear and thermal history will have a significant effect on the rheological characteristics of the melt flow. For example, at higher screw rotation speeds the molten polymer is exposed to high shear and experiences a corresponding decrease in melt viscosity due to the dependence of melt temperature on viscous energy dissipation via shearing.

So, polymer melts exhibit shear thinning or pseudoplastic flow behaviour in extrusion operations whereby an increase in shear rate causes a decrease

in melt viscosity. Figure 3.12 shows a plot of log (shear viscosity) against log (shear rate) to illustrate the general viscous behaviour of the melt flow. The flow curve is divided into three different regions.

- At low shear rate, in region I, polymers usually exhibit a Newtonian plateau which is commonly called zero-shear rate viscosity (η_0).
- In region II or region of transition, the viscosity changes non-linearly with shear rate
- In region III, the viscosity decreases with increasing shear rate, exhibiting shear thinning behaviour.

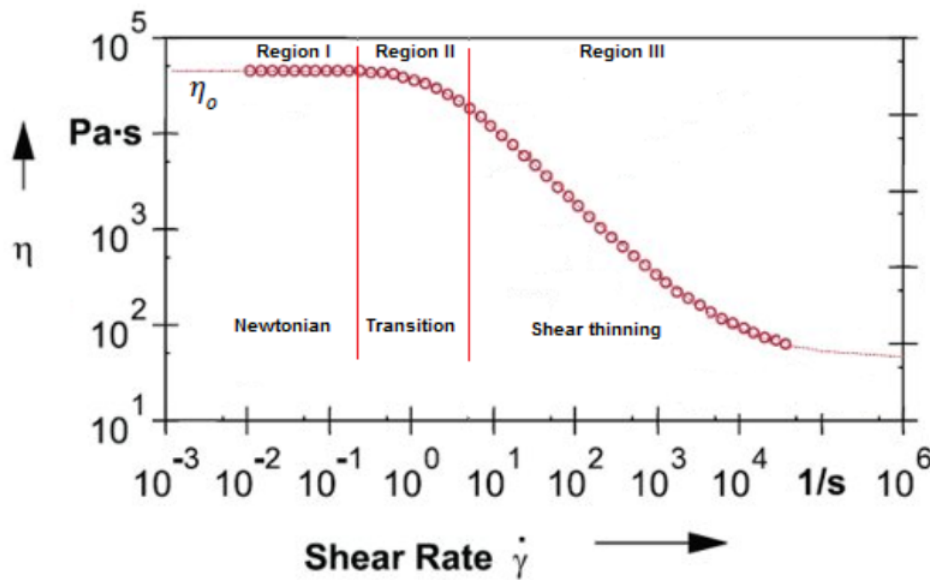


Figure 3.13: Variation of shear viscosity with shear rate for polymer melts

3.3.4 Polymer Melt Flow Rate

The plastic melt flows in three different axes of a helical system: helical (down channel), normal (radial), and tangential (cross channel).

One of the most common theoretical equations for calculating the flow rate of polymer melt in an extrusion or injection molding process is shown in the equation below [Rauwendaal 86].

The flow rate in this equation depends on drag flow [first part of the right hand side in Equation] and pressure flow [second section of Equation], where:

$$Q = W_0 \pi N R_b^3 \sin \phi \cos \phi F(\beta) - \frac{W_0 \sin^2 \phi R_b^4}{16\eta} \left[1 - \beta^4 + \frac{(1 - \beta^2)^2}{\ln \beta} \right] \frac{dP}{dz}$$

W_0 represent the angular channel width in radians, N is the screw peripheral speed in rpm, $F(\beta)$ is the ratio of the radii R_s/R_b , ϕ is the helix angle and the term dP/dz represents the pressure gradient (Pa).

3.3.5 Polymer Melt Thermal Conductivity

The melting of the polymer is carried out by heaters (external source) and internal heat from viscous energy dissipation via shearing (viscous dissipation). The heaters contribute less to the melting process, due to the poor thermal conductivity of the polymer melt. So, the main supplier of heat is the viscous dissipation and work done by the moving fluid, which is caused by the screw rotation inside the extruder. The screw rotation actually smears the molten polymer between the solid bed and the barrel wall (work-induced heat), generating shear and mechanical heat. All this dissipative heat generation and heat conduction with the barrel and screw within the melt has as a result the non-uniformity of the melt temperature inside the screw channel and melt temperature changes in all axes.

Viscous dissipation is defined as the irreversible process by means of which the work done by a fluid on adjacent layers due to the action of shear forces is transformed into heat. Therefore, viscous dissipation is always positive as it gives rise to a thermal source in the flow. Also, the thermal phenomenon in extrusion process shows a deep dependence between viscous dissipation and melt viscosity.

So, the importance of choosing the appropriate screw design is more than obvious, to ensure the optimization of the extrusion process and quality of the extruded polymer.

Chapter 4

Experimental Measurements of Extrusion Processes

4.1 Betol BC-60 Extruder

This section provides information of material and details of the experimental equipment used to carry out the experimental work by ([Abeykoon, Li, McAfee, Martin, Niu, et al., 2011](#)).

4.1.1 Material

Throughout the studies, a recycled extrusion grade black HDPE (high density polyethylene) was used (MFI -0.16g/10min, density - $0.967\text{g}/\text{cm}^3$, and $\sim 2.5\%$ carbon black) provided by Cherry Pipes Ltd. The melt flow index (MFI) value is presented according to the ISO 1133 standard (190°C, 2.16kg).

4.1.2 Experimental equipment

4.1.2.1 Large scale single screw extruder

All measurements were carried out using a 63.5 mm diameter (D) single screw extruder (Davis standard BC-60) which is shown in Figure 4.1.

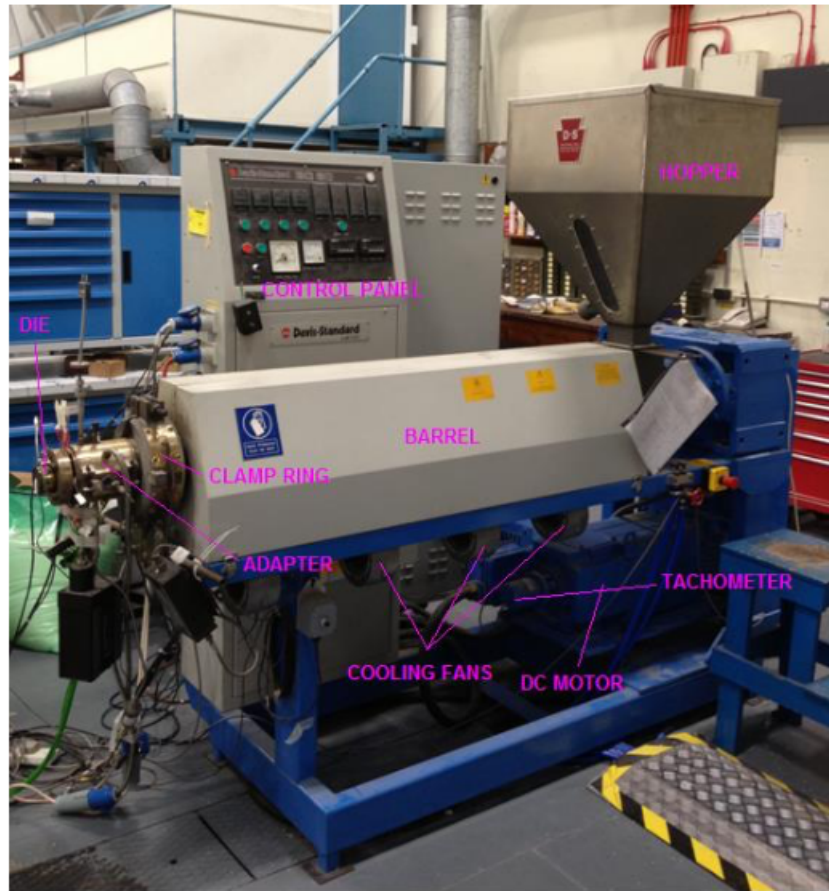


Figure 4.1: Betol BC-60 single screw extruder

The temperature along the barrel is controlled with Davis Standard Dual Therm temperature controllers and air cooling. Temperature controllers are placed along the extruder barrel arranged in four separate temperature zones and three separate temperature zones at the clamp ring, adapter and die. The extruder barrel dimensions and the arrangement of the heaters are shown in Fig. 4.2

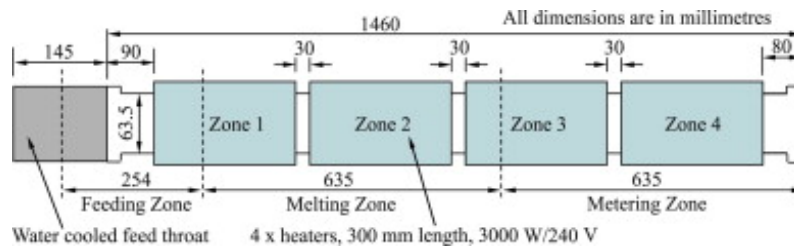


Figure 4.2: Arrangement of the Betol BC-60 extruder barrel and heaters

4.1.2.2 Screw geometry used in the large scale single screw extruder

A tapered gradual compression screw with 3:1 compression ratio was used to process polymer material. The parts of the screw are (Figure 4.3):

- Feed or solids conveying - length: $4 \times D$ and channel height: 10.53mm
- Compression or melting - length: $10 \times D$
- Metering - length: $10 \times D$ and channel height: 3.46mm

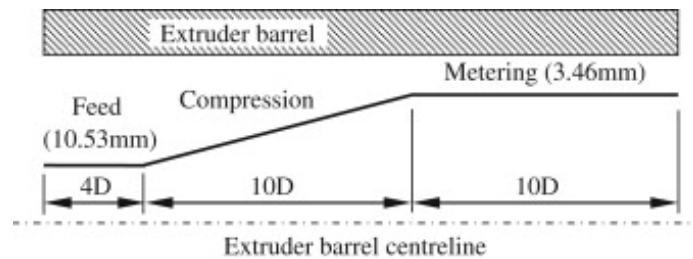


Figure 4.3: Details of the gradual compression screw

4.1.2.3 Operating conditions used in the large scale single screw extruder

Three experimental trials were carried out and denoted as: A (low temperature), B (medium temperature) and C (high temperature). Experiments were performed at a range of extruder screw speeds from 10 – 90 rpm in step sizes of 40 rpm in tests A and C and in step sizes of 20rpm in test B. Sufficient time (around 9 minutes) was allowed for conditions to stabilise at each screw speed before data were recorded. The extruder set temperatures are described below:

Test	Temperature settings (°C)						
	Barrel zones				Clamp ring	Adapter	Die
	1	2	3	4			
A	130	155	170	180	180	180	180
B	140	170	185	200	200	200	200
C	150	185	200	220	220	220	220

Table 4.1: Extruder barrel temperature settings

The six model inputs from Table 4.1 (T_1 , T_2 , T_3 , T_4 , Clamp ring, Adapter and Die) are shown in Fig. 2.1. It is clear from this figure and the Table 4.1 that the set temperatures of the clamp ring, the adapter and the die are always equal to T_4 in this study.

4.1.2.4 Monitoring techniques used in the large scale single screw extruder

In-process monitoring techniques were used to assess the extrusion process using an instrumented die adaptor (internal diameter 38mm) with a clamp ring prior to the entrance of a 12mm capillary die. Die temperature was controlled with Davis Standard Dual Therm controllers clamped to the die clamp ring, adapter and die, as mentioned before in 4.1.2.1. A schematic diagram of this measurement region is shown in Figure 4.4

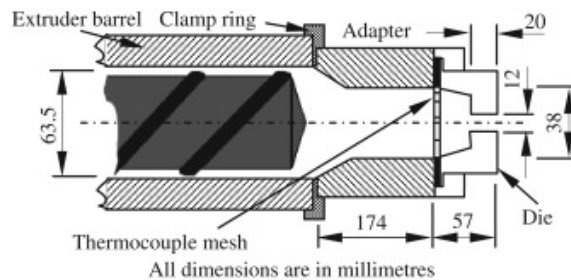


Figure 4.4: Extruder die, adapter and thermocouple mesh

Melt temperature profiles at the die were measured using a thermocouple mesh placed in-between the adapter and the die. The thermocouple sensors used by (Abeykoon, Li, McAfee, Martin, Niu, et al., 2011) have been described in detail previously (describing also the geometry of the thermocouple

mesh sensor) in "Temperature measurement methods for single screw extrusion" (section 3.3.4) and "Thermocouple mesh devices" (subsection 3.3.4.1). The final temperature profile was obtained by the 11 radial positions (distances from the die centreline to each radial position: 0 mm, ± 3 mm, ± 5 mm, ± 8.5 mm, ± 15 mm and ± 19 mm).

4.1.3 Experimental Results

The experimentally measured temperature profiles are shown in the table below along with the screw speed, the three experimental trials (A, B, C) described in 4.1.2.3, the desired average die melt temperature and the corresponding barrel set temperatures. It has to be mentioned that the set temperatures of the clamp ring, the adapter and the die are always equal to T_4 in this study and are measured at the $R_p = 0$ mm of the thermocouple mesh.

Screw speed (rpm)	Test Condition	Desired melt temperature ($^{\circ}$ C)	Barrel temperatures ($^{\circ}$ C)			
			T_1	T_2	T_3	T_4
10 (ω_1)	A	190	130	155	170	180
	B	210	140	170	185	200
	C	230	150	185	200	220
30 (ω_2)	B	215	140	170	185	200
50 (ω_3)	A	200	130	155	170	180
	B	220	140	170	185	200
	C	235	150	185	200	220
70 (ω_4)	B	225	140	170	185	200
90 (ω_5)	A	210	-	-	-	-
	B	230	140	170	185	200
	C	245	150	185	200	220

Table 4.2: Experimentally measured temperature profiles

As it is obvious, no experimental data were available for some specific test conditions and screw speeds, due to a broken mesh junction through the experiment.

4.2 Husky IMS Injection Machine

This section provides information of material and details of the experimental equipment used to carry out the experimental work by (Sanjabi, 2010).

4.2.1 Material

Throughout the studies, the experiment was held in 3 different situations:

- **HDPE WITH GENERAL PURPOSE SCREW** A HDPE resin with MFI of 2g/10min and a general purpose screw (GP).
- **HDPE WITH BARRIER SCREW** The same HDPE resin as above was used here, but the screw type changed to a Barrier screw.
- **PET WITH PET SCREW** A PET resin with intrinsic viscosity (IV) of 0.83 dl/g and a PET screw were utilized in this situation.

More detailed information about these 3 situations can be found in section 2.1 "Melt Temperature".

4.2.2 Experimental equipment

All measurements were carried out using a single screw injection molding machine manufactured by Husky IMS, which is shown in Figure 4.5.

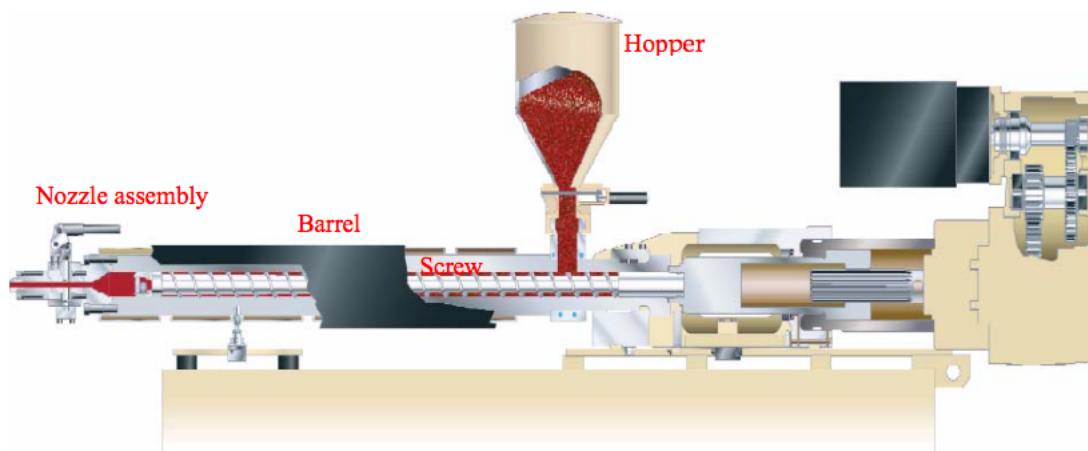


Figure 4.5: A schematic of a single screw Husky IMS injection machine

4.2.2.1 Monitoring techniques used in Husky IMS Injection Machine

The extruder was instrumented with control hardware to measure the melt pressure at the screw tip (Kistler 6081A pressure transducer), and thermocouple to measure the melt temperature at the machine nozzle location

(Dynisco TG422J). The location of the temperature and pressure sensors are shown in Figure 4.6. The screw torque and the heater power draw were obtained from the motor amperage indicated by the machine control system.

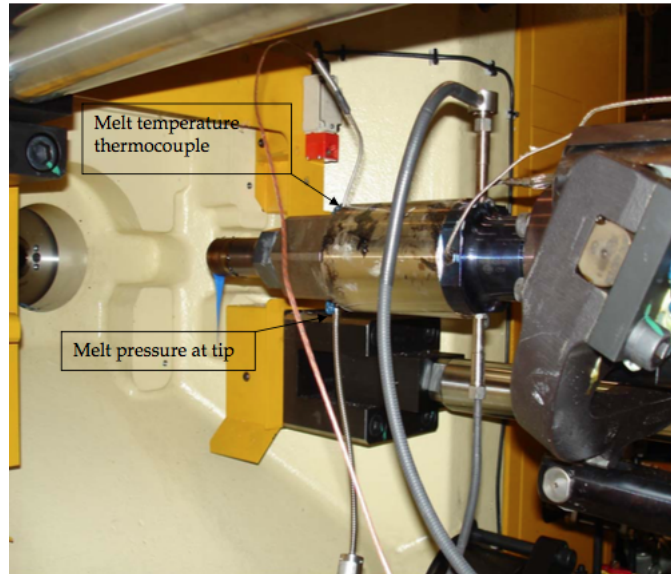


Figure 4.6: Location of the melt pressure and temperature sensors at the injection unit

4.2.2.2 Screw geometry used in Husky IMS Injection Machine

As it was analyzed in full detail in section 2.1, screw designs used in this experiment include:

- **GENERAL PURPOSE SCREW** for processing high density polyethylene
- **BARRIER SCREW** for processing high density polyethylene
- **PET SCREW** for processing of PET resins

All screws had outside diameter of 80 mm and length of 25:1 L/D. Due to the confidentiality agreements with Husky Injection Molding Systems Ltd., the configuration of the screw designs were not shown in (Sanjabi, 2010) study.

4.2.2.3 Operating conditions used in Husky IMS Injection Machine

Ten experimental runs were carried out: four with the General Purpose screw (using HDPE), four with the barrier screw (using HDPE) and two with the PET screw (using PET). The inputs to the experiments are described to the table 4.3 below:

Run	Resin	Barrel temp (°C)	Screw speed (rpm)
1	HDPE MFI = 2g/10min GP (25:1)	210	190
2			286
3		230	190
4			286
5	HDPE MFI = 2g/10min Barrier (25:1)	210	190
6			286
7		230	190
8			286
9	PET, IV = 0.83dl/g PET (25:1)	285	285
10		300	300

Table 4.3: Design of experiment (experiment inputs)

4.2.3 Experimental Results

Below in Table 4.4 are presented the experimental results for the 10 runs

Run	Resin	Barrel temp (°C)	Screw speed (rpm)	Recovery time (sec)	Melt temp (°C)	Torque (Nm)	Shot weight (g)	Nozzle pressure (bar)
1	HDPE MFI=2g/10min GP (25:1)	210	190	1.76	244.2	4402	180	1149.6
2			286	1.36	245.0	4874	240	1135.0
3		230	190	1.76	253.0	4239	180	1113.0
4			286	1.36	252.8	4656	240	1101.0
5	HDPE MFI=2g/10min Barrier (25:1)	210	190	1.76	245.3	4402	180	1149.6
6			286	1.36	245.9	4874	240	1135.0
7		230	190	1.76	254.1	4239	180	1113.0
8			286	1.36	255.2	4656	240	1101.0
9	PET, IV=0.83dl/g PET (25:1)	285	300	2.70	299.3	8803	640	-
10		300		3.10	306.4	8085	640	-

Table 4.4: Experimental Results
(Sanjabi, 2010)

Shot weight is referring to **shot size**, which is the maximum amount of plastic injection mold that can be injected in one molding cycle.

During the screw recovery in injection molding, the screw is pulled back to allow certain volume of melt to be collected in front of its tip. This volume is referred to as *shot size*.

Figure 4.7 depicts the shot size in extrusion process. In this example there is 2 L/D of screw available (as the screw contains 25 L/D units and the desired bulk temperature occurs at L/D = 23 of the screw), which can be added to the shot size related to this process. So, there is 2 L/D volume of melt available in each cycle, which might either improve or degrade the melt before exiting the injection barrel.

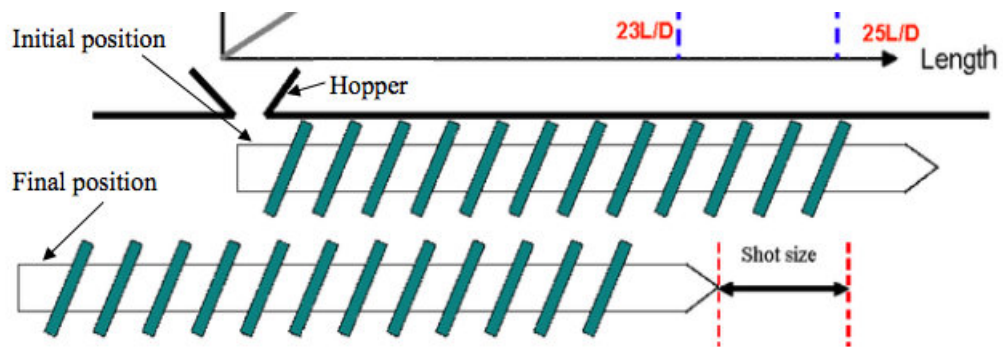


Figure 4.7: Visual explanation of shot size in the extrusion process, with linear motion of the screw shown

Shot size can offer to more production opportunity, if used in the right amount. Smaller shot sizes produce greater irregularities and loss of precision, whereas larger shot sizes do not allow sufficient melt cushion for packing and for inefficiencies in plastication.

Chapter 5

Basics for Regression Models

5.1 Introduction

Regression is a supervised learning method, which is employed to model and analyze the relationship between a dependent (response) variable and one or more independent variables (predictor). One can use regression to build a prediction model, which can first be used to find the best fitted model with minimum squared errors of the fitted values. The fitted model can then be further applied to data for continuous value predictions. (Bhatia & Yu-Wei, 2017)

Regression analysis is an important tool for modeling and analyzing data. There are multiple benefits of using regression analysis, like that it indicates the significant relationships between dependent variable and independent variable and also the strength of impact of multiple independent variables on a dependent variable.

There are many different types of regression. Some most commonly used in polymer extrusion models are:

- **Linear Regression:** This is the oldest type and most widely known type of regression. In this the dependent variable is continuous and the independent variable can be discrete or continuous and the regression line is linear. Linear regression is very sensitive to outliers and cross-correlations.
- **Polynomial Regression:** This implies of polynomial equation here the power of the independent variable is more than one. In this case the regression line is not a straight line, but a curved line.
- **Linear Least Squares Regression and Multiple Linear Regression:** which will be described in full detail right below.

5.2 Linear Least Squares Regression

Linear least squares (LLS) regression is the most widely used modeling method. It has also been adapted to a broad range of situations that are outside its direct scope. The linear least squares fitting technique is the simplest and most commonly applied form of linear regression and provides a solution to the problem of finding the best fitting straight line through a set of points.

Linear least squares regression can be used to fit the data with any function of the form:

$$f(\vec{x}; \vec{\beta}) = \beta_0 + \beta_1 x_1 + \beta_2 x_2 + \dots \quad (5.1)$$

in which each explanatory variable in the function is multiplied by an unknown parameter, there is at most one unknown parameter with no corresponding explanatory variable and all of the individual terms are summed to produce the final function value.

In statistical terms, any function that meets these criteria would be called a "linear function". The term "linear" is used, even though the function may not be a straight line, because if the unknown parameters are considered to be variables and the explanatory variables are considered to be known coefficients corresponding to those "variables", then the problem becomes a system (usually overdetermined) of linear equations that can be solved for the values of the unknown parameters.

Linear least squares regression also gets its name from the way the estimates of the unknown parameters are computed. This is the "method of least squares" that is used to obtain parameter estimates. In the least squares method the unknown parameters are estimated by minimizing the sum of the squared deviations between the data and the model. The minimization process reduces the overdetermined system of equations formed by the data to a sensible system of p (where p is the number of parameters in the functional part of the model) equations in p unknowns. This new system of equations is then solved to obtain the parameter estimates.

5.3 Multiple Linear Regression

A simple linear regression is a function where a single predictor variable X was used to model the response variable Y . Linear regression can only be used when one has two continuous variables – an **independent** variable and a **dependent** variable. The independent variable is the parameter that is used to calculate the dependent variable or outcome.

In reality, there are multiple factors that predict the outcome of an event. To understand a relationship in which more than two variables are present, a multiple linear regression is used. Multiple regression models thus describe how a single response variable Y depends linearly on a number of predictor variables.

Multiple linear regression (MLR) is used to determine a mathematical relationship among a number of random variables. In other terms, MLR examines how multiple independent variables are related to one dependent variable. Once each of the independent factors have been determined to predict the dependent variable, the information on the multiple variables can be used to create an accurate prediction on the level of effect they have on the outcome variable. The model creates a relationship in the form of a straight line (linear) that best approximates all the individual data points.

A multiple linear regression model can be written as:

$$\hat{Y} = \beta_0 + \beta_1 X_1 + \beta_2 X_2 + \dots + \beta_p X_p + \epsilon \quad (5.2)$$

where ϵ is the random error in prediction that is variance that cannot be accurately predicted by the model (known as residuals), \hat{Y} is the predicted or expected value of the dependent variable, X_1 through X_p are p distinct independent or predictor variables, β_0 is the value of Y when all of the independent variables (X_1 through X_p) are equal to zero, and β_1 through β_p are the estimated regression coefficients. Each regression coefficient represents the change in Y relative to a one unit change in the respective independent variable. In the multiple regression situation, β_1 , for example, is the change in Y relative to a one unit change in X_1 , holding all other independent variables constant (i.e., when the remaining independent variables are held at the same value or are fixed). Statistical tests can be performed to assess whether each regression coefficient is significantly different from zero.

5.4 Regression Diagnostics

Regression diagnostics are used to evaluate the model assumptions and investigate whether or not there are observations with a large, undue influence on the analysis. The assumptions for linear regression are:

- **LINEARITY:** the relationships between the predictors and the outcome variable should be linear. *Big deal if violated.*
- **NORMALITY:** the errors should be normally distributed – normality is necessary for the b-coefficient tests to be valid (especially for small samples), estimation of the coefficients only requires that the errors be

identically and independently distributed. *Not as big of a deal if violated.*

- **HOMOSCEDASTICITY:** the error variance should be constant. *Not as big deal if violated.*
- **NO OR LITTLE MULTICOLLINEARITY:** predictors that are highly related to each other and both predictive of your outcome, can cause problems in estimating the regression coefficients.
- **INDEPENDENCE:** the errors associated with one observation are not correlated with the errors of any other observation. *Huge deal if violated!*

5.5 Measuring Performance in Regression Models

For models predicting a numeric outcome, some measure of accuracy is typically used to evaluate the effectiveness of the model. The most common method for characterizing a model's predictive capabilities when the outcome is a number, is to use the **root mean squared error (RMSE)**. This metric is a function of the model residuals, which are the observed values minus the model predictions. The mean squared error (MSE) is calculated by squaring the residuals, summing them and dividing by the number of samples. The RMSE is then calculated by taking the square root of the MSE so that it is in the same units as the original data. The value is usually interpreted as either how far (on average) the residuals are from zero or as the average distance between the observed values and the model predictions.

Another common metric is the **coefficient of determination**, commonly written as R^2 . This value can be interpreted as the proportion of the information in the data that is explained by the model. So R^2 is a measure of correlation, not accuracy. There are multiple formulas for calculating this quantity, although the simplest version finds the correlation coefficient between the observed and predicted values (usually denoted by R) and squares it. (Kuhn & Johnson, 2013)

There are also some performance metrics that represent a more intuitive concept of model's performance.

Mean Absolute Deviation (MAD) measures the size of the error in units. MAD takes the absolute value of forecast errors and averages them over the entirety of the forecast time periods. Taking an absolute value of a number disregards whether the number is negative or positive and, in this case, avoids the positives and negatives canceling each other out. MAD is obtained by using the following formula:

$$MAD = \frac{1}{n} \sum_{i=1}^n |x_i - \bar{x}| \quad (5.3)$$

Mean Absolute Percentage Error (MAPE) measures the size of the error in percentage terms. MAPE is the average absolute percent error for each time period or forecast minus actuals divided by actuals:

$$MAPE = \frac{100\%}{n} \sum_{t=1}^n \left| \frac{A_t - F_t}{A_t} \right| \quad (5.4)$$

where A_t is the actual value and F_t is the forecast value.

5.6 Model Evaluation

Model evaluation is performed to ensure that a fitted model can accurately predict responses for future or unknown subjects. Without model evaluation, we might train models that over-fit in the training data.

Whenever we are building a model, it needs to be tested and evaluated to ensure that it will not only work on trained data, but also on unseen data and can generate results with accuracy. A model should not generate a random result though some noise is permitted. If the model is not evaluated properly then the chances are that the result produced with unseen data is not accurate. Furthermore, model evaluation can help select the optimum model, which is more robust and can accurately predict responses for future subjects. There are various ways by which a model can be evaluated ([Bhatia & Yu-Wei, 2017](#)):

- **SPLIT TEST:** In a split test, the dataset is divided into two parts, one is the training set and the other is test dataset. Once data is split the algorithm will use the training set and a model is created. The accuracy of a model is tested using the test dataset. The ratio of dividing the dataset in training and test can be decided on basis of the size of the dataset. It is fast and great when the dataset is of large size or the dataset is expensive. It can produce different result on how the dataset

is divided into the training and test dataset. If the date set is divided in 80% as a training set and 20% as a test set, 60% as a training set and 40%, both will generate different results. We can go for multiple split tests, where the dataset is divided in different ratios and the result is found and compared for accuracy.

- **CROSS VALIDATION:** In cross validation, the dataset is divided in number of parts, for example, dividing the dataset in 10 parts. An algorithm is run on 9 subsets and holds one back for test. This process is repeated 10 times. Based on different results generated on each run, the accuracy is found. It is known as k-fold cross validation is where k is the number in which a dataset is divided. Selecting the k is very crucial here, which is dependent on the size of dataset.
- **BOOTSTRAP:** This starts with some random samples from the dataset, and an algorithm is run on dataset. This process is repeated for n times until we have all covered the full dataset. In aggregate, the result provided in all repetition shows the model performance.
- **LEAVE ONE OUT CROSS VALIDATION:** As the name suggests, only one data point from the dataset is left out, an algorithm is run on the rest of the dataset and it is repeated for each point. As all points from the dataset are covered it is less biased, but it requires higher execution time if the dataset is large.

5.7 Analysis of Variance (ANOVA)

The acronym **ANOVA** refers to **analysis of variance** and is a statistical procedure used to test the degree to which two or more groups vary or differ in an experiment. It tests whether the means of various groups are equal or not. In ANOVA, the variance observed in a particular variable is partitioned into different components based on the sources of variation. An important fact to note is that while we use ANOVA to find out whether the means differ significantly, we actually compare the variances (hence the name - ANalysis Of Variance)

There are two types of analysis of variance: one-way (or unidirectional) and two-way. One-way or two-way refers to the number of independent variables in your Analysis of Variance test. A one-way ANOVA evaluates the impact of a sole factor on a sole response variable. It determines whether all the samples are the same. The one-way ANOVA is used to determine

whether there are any statistically significant differences between the means of three or more independent (unrelated) groups.

A two-way ANOVA is an extension of the one-way ANOVA. With a one-way, you have one independent variable affecting a dependent variable. With a two-way ANOVA, there are two independents. It tests the effect of two factors at the same time.

In our research we will need the one-way ANOVA. The one-way ANOVA compares the means between the interested groups and determines whether any of those means are statistically significantly different from each other. Specifically, it tests the null hypothesis:

$$H_0 : \mu_1 = \mu_2 = \mu_3 = \dots = \mu_K \quad (5.5)$$

where μ = group mean and k = number of groups. If, however, the one-way ANOVA returns a statistically significant result, we accept the alternative hypothesis (H_A), which is that there are at least two group means that are statistically significantly different from each other.

Last but not least, a refer to MANOVA has to be made. Multivariate analysis of variance (MANOVA) is simply an ANOVA with several dependent variables. That is to say, ANOVA tests for the difference in means between two or more groups, while MANOVA tests for the difference in two or more vectors of means.

5.8 Principal Component Analysis (PCA)

Multivariate Analysis often starts out with data involving a substantial number of correlated variables. Principal Component Analysis (PCA) is a dimension-reduction tool that can be used to reduce a large set of variables to a small set that still contains most of the information in the large set.

Principal component analysis (PCA) is a statistical procedure that uses an orthogonal transformation to convert a set of observations of possibly correlated variables into a set of values of linearly uncorrelated variables called *principal components*. The first principal component accounts for as much of the variability in the data as possible, and each succeeding component accounts for as much of the remaining variability as possible.

PCA can be thought of as fitting an n-dimensional ellipsoid to the data, where each axis of the ellipsoid represents a principal component. If some axis of the ellipsoid is small, then the variance along that axis is also small, and by omitting that axis and its corresponding principal component from our representation of the dataset, we lose only a commensurately small amount of information.

To find the axes of the ellipsoid, we must first subtract the mean of each variable from the dataset to center the data around the origin. Then, we compute the covariance matrix of the data, and calculate the eigenvalues and corresponding eigenvectors of this covariance matrix. Then we must normalize each of the orthogonal eigenvectors to become unit vectors. Once this is done, each of the mutually orthogonal, unit eigenvectors can be interpreted as an axis of the ellipsoid fitted to the data. This choice of basis will transform our covariance matrix into a diagonalised form with the diagonal elements representing the variance of each axis. The proportion of the variance that each eigenvector represents can be calculated by dividing the eigenvalue corresponding to that eigenvector by the sum of all eigenvalues.

This procedure is sensitive to the scaling of the data, and there is no consensus as to how to best scale the data to obtain optimal results. (PCA, n.d.)

5.9 Comparison of ANOVA and Regression

ANOVA and regression are like the flip sides of the same coin. They are different, but they have more in common than you might think at first glance. These two are closely related and we can formulate ANOVA problems as regression problems or analyse regression problems using ANOVA.

A very simple explanation is that regression is the statistical model that you use to predict a continuous outcome on the basis of one or more continuous predictor variables. In contrast, ANOVA is the statistical model that you use to predict a continuous outcome on the basis of one or more categorical predictor variables. Although these two are different, both models are applicable only when you have a continuous outcome variable.

We use regression when the independent variables are measured on a quantitative scale. Sometimes the independent variables may be of both kinds, some qualitative, some quantitative. In this case we can carry out a combined analysis called **analysis of covariance (ANCOVA)**, in which the covariates are the quantitative variables.

In fact, we can go further and treat ANOVA, regression and the combination, ANCOVA, as particular cases of a wider approach called **generalized linear modelling**. It is important, however, to be clear as to just what each technique does and it is useful to think of ANOVA and regression as separate but related techniques.

Interaction effects occur when the effect of one variable depends on the value of another variable. The concept of interactions applies to regression just as to ANOVA. (In regression problems we simply include new variables

that are products of the original variables)

(Williams, 2017) claim the use of weights in ANOVA and regression as an important extension of these ideas, as it is really common to have data for which the different points are measured with differing accuracy. In regression analysis heteroscedasticity means a situation in which the variance of the dependent variable (Y) varies across the levels of the independent data (X). Heteroscedasticity can complicate analysis because regression analysis is based on an assumption of equal variance across the levels of the independent data. Weighted regression can be used to correct for heteroscedasticity. In a Weighted regression procedure more weight is given to the observations with smaller variance because these observations provide more reliable information about the regression function than those with large variances. It works by incorporating extra nonnegative constants, or weights, associated with each data point, into the fitting criterion. So, instead of finding the model that minimizes the sum of the squares of the residuals $\sum \epsilon_i^2$, we find the model that minimizes $\sum \epsilon_i^2 w_i$ where we choose the weights w_i so that the more precise observations are given greater weight than the less precise observations. R-Square

5.10 SPSS Program

SPSS is a widely used program for statistical analysis. The base software includes:

- **DESCRIPTIVE STATISTICS:** Cross tabulation, Frequencies, Descriptives, Explore, Descriptive Ratio Statistics
- **BIVARIATE STATISTICS:** Means, t-test, ANOVA, Correlation (bivariate, partial, distances), Nonparametric tests, Bayesian
- **PREDICTION FOR NUMERICAL OUTCOMES:** Linear regression
- **ETC.**

In this thesis, SPSS will be used for building a model based on Multiple Linear Regression which computes the final desired temperature of the melt, based on the temperature barrel input and the screw speed.

To prove Multiple Linear Regression assumptions, SPSS offers some plots:

- **SCATTERPLOT:** A simple scatterplot can be used to (a) determine whether a relationship is linear, (b) detect outliers and (c) graphically present a relationship.

In our case, we use scatterplot of Studentized Residuals and Deleted Studentized Residuals. These are commonly used for identifying outliers.

- **PARTIAL REGRESSION PLOT:** When performing a linear regression with a single independent variable, a scatter plot of the response variable against the independent variable provides a good indication of the nature of the relationship.
- **HISTOGRAMS:** A histogram is a plot that lets you discover and show, the underlying frequency distribution (shape) of a set of data. It is commonly used for checking normality in SPSS. Plotting a histogram of the variable of interest will give an indication of the shape of the distribution. A normal approximation curve can also be added by editing the graph.
- **NORMAL P-P PLOT:** A normal probability plot is extremely useful for testing also normality assumptions. It's more precise than a histogram. The P-P plot plots the corresponding areas under the curve (cumulative distribution function) for those values.

More detailed work will be found in Chapter 6.

5.11 The basics of Neural Network (NN)

Neural Network concept relies on how the brain works. In simple terms, the brain is composed of large numbers of interconnected neurons working together to solve a specific problem. Neurons, in turn, are inter-connected with dendrites that produce output signals based on the inputs through an axon to another neuron. Neural nets are used to teach or rather a computer learns to perform a task by analyzing some training examples provided, like object or pattern recognition.

The neural network is a network made up of artificial neurons (or nodes). There are three types of neurons within the network: input neurons, hidden neurons, and output neurons. In the network, neurons are connected; the connection strength between neurons is called weight. If the weight is greater than zero, it is in an excitation status. Otherwise, it is in an inhibition status. Input neurons receive the input information; the higher the input value, the greater the activation. Then, the activation value is passed through the network in regard to weights and transfer functions in the graph. The hidden neurons (or output neurons) then sum up the activation values and modify

the summed values with the transfer function. The activation value then flows through hidden neurons and stops when it reaches the output nodes. As a result, one can use the output value from the output neurons to classify the data.

The advantages of a neural network are: First, that it can detect nonlinear relationships between the dependent and independent variable. Second, one can efficiently train large datasets using the parallel architecture. Third, it is a nonparametric model so that one can eliminate errors in the estimation of parameters.

The main disadvantages of a neural network are that it often converges on the local minimum, rather than the global minimum. Also, it might over-fit when the training process goes on for too long. (Bhatia & Yu-Wei, 2017)

5.12 Nonlinear Regression using ANFIS

Adaptive Neuro-Fuzzy Inference System (ANFIS) is a multilayer feed-forward network which is used to scheme an input space to an output space by incorporation of artificial neural network (ANN learning algorithms) and fuzzy logic (Takagi-Sugeno-type fuzzy system) and it is proposed by (Jang, 1993). ANFIS inherits the benefits of both neural networks and fuzzy systems; so it is a powerful tool for doing various supervised learning tasks, such as regression and classification.

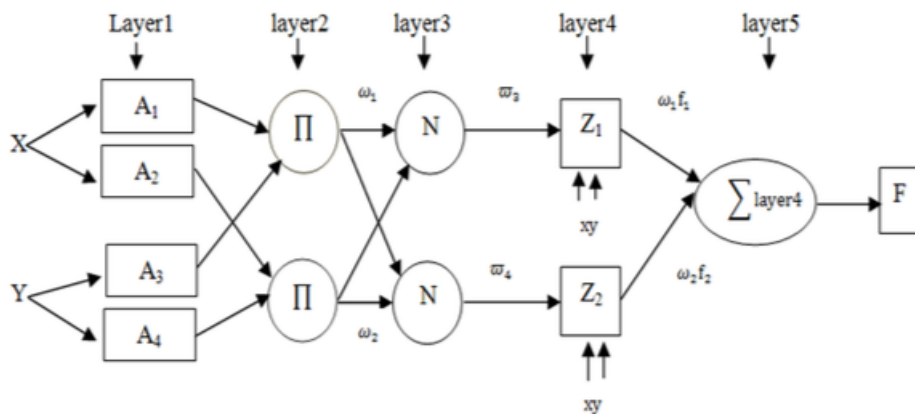


Figure 5.1: Adaptive neuro-fuzzy inference system structure

As can be seen in Figure 5.1, a typical ANFIS structure is including five layers. The first layer consists of membership functions (MFs). The most common MF encompasses bell-shaped, Gaussian and triangular. The second

layer calculates the firing robustness of a rule multiplication. The third layer indicates outputs called normalized firing strengths. The output of the fourth layer is composed of a linear combination of the inputs multiplied by the normalized firing strength ω . The fifth layer is the simple summation of the outputs of the fourth layer. ([Elhami, Akram, Khanali, & Mousavi-Avval, 2016](#))

Chapter 6

Proposed Mathematical Modeling of the Die Melt Temperature Profile

As it was not possible to have my own experimental results in order to model the die melt temperature profile through a single screw extruder, I used experimental results from ([Abeykoon et al., 2010](#)) study for the training and validation data of my models.

6.1 Experimental Inputs for the Models creation (Missing Data filling)

My main aim was to **model the effects of process settings on the shape of the die melt temperature profile.**

The concept in which I was based to create 2 different models is that the melt temperature profile at the die ($T_{p,die}$) can be represented as a function of ω_{sc} and T_b :

$$T_{p,die} = f(\omega_{sc}, T_b) \quad (6.1)$$

where ω_{sc} is the screw speed and T_b represents the barrel set temperatures at different zones (T_1, T_2, T_3, T_4). For simplicity reasons, I only used T_4 (which represents the set temperature of the clamp ring, the adapter and the die) for the input T_b , in order to eliminate the inputs and simplify my models.

From these 3 variables, ω_{sc} and T_b are independent variables and $T_{p,die}$ is the dependent variable.

So for the first phase, the model creation, I used the experimental results from (Abeykoon et al., 2010) that are in Table 4.1 in section 4.1.3. Because I used only T_4 from my barrel temperatures, the table gets like this:

Screw speed (rpm)	Test Condition	Desired melt temperature (°C)	Barrel temperatures (°C)
			T_4
10 (ω_1)	A	190	180
	B	210	200
	C	230	220
30 (ω_2)	B	215	200
50 (ω_3)	A	200	180
	B	220	200
	C	235	220
70 (ω_4)	B	225	200
90 (ω_5)	A	210	-
	B	230	200
	C	245	220

Table 6.1: Experimental melt temperature profile table, using only T_4 for T_b

Then, I sorted the data from Table 6.1 based on desired melt temperature for all screw speeds and the result was this:

		Desired melt temperature (°C)								
		190	200	210	215	220	225	230	235	245
Screw Speed (rpm)	10 (ω_1)	180	-	200	-	-	-	220	-	-
	30 (ω_2)	-	-	-	200	-	-	-	-	-
	50 (ω_3)	-	180	-	-	200	-	-	220	-
	70 (ω_4)	-	-	-	-	-	200	-	-	-
	90 (ω_5)	-	-	180	-	-	-	200	-	220

Table 6.2: Experimental melt temperature profile table with order based on desired melt temperature for all the screw speeds

As it's obvious, there are many null cells on the Table 6.2 and I want all my table full of elements so I can then compute my models. I used Matlab to find the missing data in my sample. Here's the code I used:

```

% for w1 = 10rpm
x = {190 200 210 215 220 225 230 235 245};
y = {180 NaN 200 NaN NaN NaN 220 NaN NaN};
x=cell2mat(x);
y=cell2mat(y);
xi=x(find(~isnan(y)));
yi=y(find(~isnan(y)))
result1=interp1(xi,yi,x,'spline','extrap')

%for w2 = 50rpm
x = {190 200 210 215 220 225 230 235 245};
y = {NaN 180 NaN NaN 200 NaN NaN 220 NaN};
x=cell2mat(x);
y=cell2mat(y);
xi=x(find(~isnan(y)));
yi=y(find(~isnan(y)))
result2=interp1(xi,yi,x,'spline','extrap')

%for w3 = 90rpm
x = {190 200 210 215 220 225 230 235 245};
y = {NaN NaN 180 NaN NaN NaN 200 NaN 220};
x=cell2mat(x);
y=cell2mat(y);
xi=x(find(~isnan(y)));
yi=y(find(~isnan(y)))
result3=interp1(xi,yi,x,'spline','extrap')

```

I found the missing numbers by using function `interp1`. More specifically, I used 'extrap' which specifies a strategy for evaluating points that lie outside the domain of `x` ('extrap' stands for the method algorithm for extrapolation). I used this function for $\omega_1, \omega_3, \omega_5$ (that had 3 elements filled in Table 6.2 each) For ω_2, ω_4 (that had only 1 element filled in Table 6.2 each) I couldn't use this function. I found their elements by calculating the mean value of ω_{x-1} and ω_{x+1} , for every column of Table 6.2 (that is for every desired temperature). The final, filled table is:

		Desired melt temperature (°C)								
		190	200	210	215	220	225	230	235	245
Screw Speed (rpm)	10 (ω_1)	180	190	200	205	210	215	220	225	235
	30 (ω_2)	176.43	185	195	200	205	210	216.43	222.5	235
	50 (ω_3)	172.86	180	189.05	194.29	200	206.19	212.86	220	235.71
	70 (ω_4)	170.24	175	185	190	195	200	206.43	213	230
	90 (ω_5)	167.62	172.86	180	184.29	189.05	194.29	200	206.19	220

Table 6.3: Final experimental melt temperature profile table. All the null cells (the red ones here) were filled with Matlab script

So Table 6.3 is the input I used for creating 2 models that show the effects of process settings (screw speed, barrel temperature) on the flow melt quality.

6.2 Die Melt Temperature Profile Models

6.2.1 Arrhenius Model based on Linear Least Squares Regression

For this model, I used the Arrhenius model for reaction rate (as the nature of my problem is Arrhenius type), took the logarithm of it and solve my model using **Linear Least Squares Regression** with Matlab. The Arrhenius model for reaction rate is:

$$r = k_0 e^{-E/RT} C^n \quad (6.2)$$

In our case T stands for barrel temperature settings (T_4), C stands for screw speed (ω_{sc}) and r stands for desired melt temperature ($T_{p,die}$). So in our case, Equation 6.2 is:

$$T_{p,die} = k_0 e^{-E/RT_4} \omega_{sc}^n \quad (6.3)$$

The logarithm of the Arrhenius type, is:

$$\ln(T_{p,die}) = \ln(k_0) + \left(-\frac{E}{R}\right) \frac{1}{T_4} + n \ln(\omega_{sc}) \quad (6.4)$$

If I write $\ln(T_{p,die})$ equal to y, $1/T_4$ equal to x_1 and $\ln(\omega_{sc})$ equal to x_2 it is obvious that the logarithm of Arrhenius model is of Linear Least Squares Regression form, where β_0 is nothing but $\ln(k_0)$, β_1 is nothing but $-(E/R)$ and β_2 is nothing but n .

To fit my data into the Arrhenius equation (and the logarithm version of it) every temperature I have has to be converted in Kelvin. So, Table 6.4 shows the converted in Kelvin table of experimental melt temperature profile.

		Desired melt temperature (Kelvin)								
		463.15	473.15	483.15	488.15	493.15	498.15	503.15	508.15	518.15
Screw Speed (rpm)	10 (ω_1)	453.15	463.15	473.15	478.15	483.15	488.15	493.15	498.15	508.15
	30 (ω_2)	449.58	458.15	468.15	473.15	478.15	483.15	489.58	495.65	508.15
	50 (ω_3)	446.01	453.15	462.20	467.44	473.15	479.34	486.01	493.15	508.86
	70 (ω_4)	443.39	448.15	458.15	463.15	468.15	473.15	479.58	486.15	503.15
	90 (ω_5)	440.77	446.01	453.15	457.44	462.20	467.44	473.15	479.34	493.15

Table 6.4: Experimental melt temperature profile table converted in Kelvin

I used Matlab to find the model. Here's the code I used:

```
% Calculate Parameters for Arrhenius Equation
% Data for speed rates

Tnew = [453.15 463.15 473.15 478.15      483.15
        488.15 493.15 498.15      508.15
        449.58 458.15 468.15 473.15      478.15
        483.15 489.58 495.65      508.15
        446.01 453.15 462.20 467.44      473.15
        479.34 486.01 493.15      508.86
        443.39 448.15 458.15 463.15      468.15
        473.15 479.58 486.15      503.15
        440.77 446.01 453.15 457.44      462.20
        467.44 473.15 479.34      493.15];

w = [10; 30; 50; 70; 90];
T = [463.15; 473.15; 483.15; 488.15; 493.15; 498.15;
     503.15; 508.15; 518.15];
w = repmat(w,9,1);
T = reshape(repmat(T',5,1),45,1);
xData = [w, T];
yData = reshape(Tnew,45,1);
clear Tnew w T

%% Linear Least Squares
x = 1./xData(:,2);
u = log(xData(:,1));
y = log(yData);
N = length(y);
```

```

X = [ones(N,1), x, u];
Y = y;
phi = inv(X'*X) * X'*Y;
% Arrhenius
k0 = exp(phi(1));
EbyR = -phi(2);
n = phi(3);

```

The matlab script gave these results:

$\mathbf{E/R} = 526,3758$

$\mathbf{k_0} = 1446,2$

$\mathbf{n} = -0.0164$

So, the die melt temperature profile model based on Arrhenius model and Linear Least Squares Regression is:

$$T_{p,die} = 1446.2e^{-526.3758*T_4}\omega_{sc}^{-0.0164} \quad (6.5)$$

6.2.2 Model based on Multiple Linear Regression

To create this model, I used IBM SPSS tool for a thorough Multiple Linear Regression analysis. I want to make sure the main assumptions are satisfied (as they were described in Chapter 5.2) in order to have reliable and valid results. After that I will find the equation of my MLR model.

In order to create my model, I inserted the data from Table 6.3 but I also inserted a new variable called Cases, which actually counts every possible combination of my other variables (so I have 45 Cases variables totally)

Note: For this section, **DV** is a shortcut of **Dependent Variable** and **IV** is a shortcut of **Independent Variable**. All SPSS tools and plots used here are described in Chapter 5.6

Assumption #1: Linearity

The first assumption of Multiple Regression is if there is a linear relationship between the DV and each one of the IVs. So, in other words, if the relationship between the IVs and the DV can be characterised by a straight line. A simple way to check this is by producing *partial regression plots* of the relationship between each of our IVs and our DV.

So, for the first Partial Regression plot, I see the relationship between the DV $T_{p,die}$ and the IV ω_{sc} :

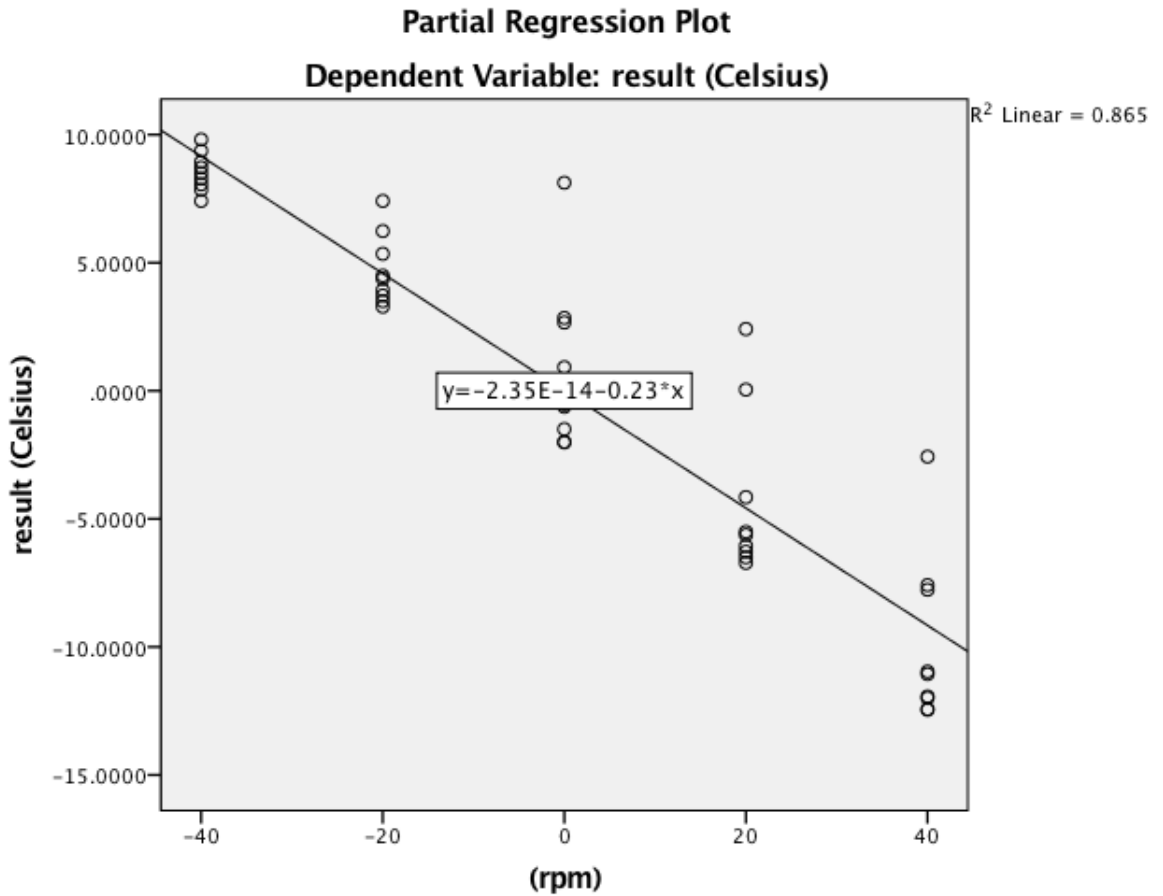


Figure 6.1: Partial Regression Plot of DV $T_{p,die}$ and IV ω_{sc}

It is obvious that the data points approximately fall to the line. The Correlation Coefficient R^2 is equal to 0.865 and so $R \approx 0.93$, which means that there is a strong linear relationship between $T_{p,die}$ and ω_{sc} .

For the second Partial Regression plot, the relationship between the DV $T_{p,die}$ and the IV T_b is:

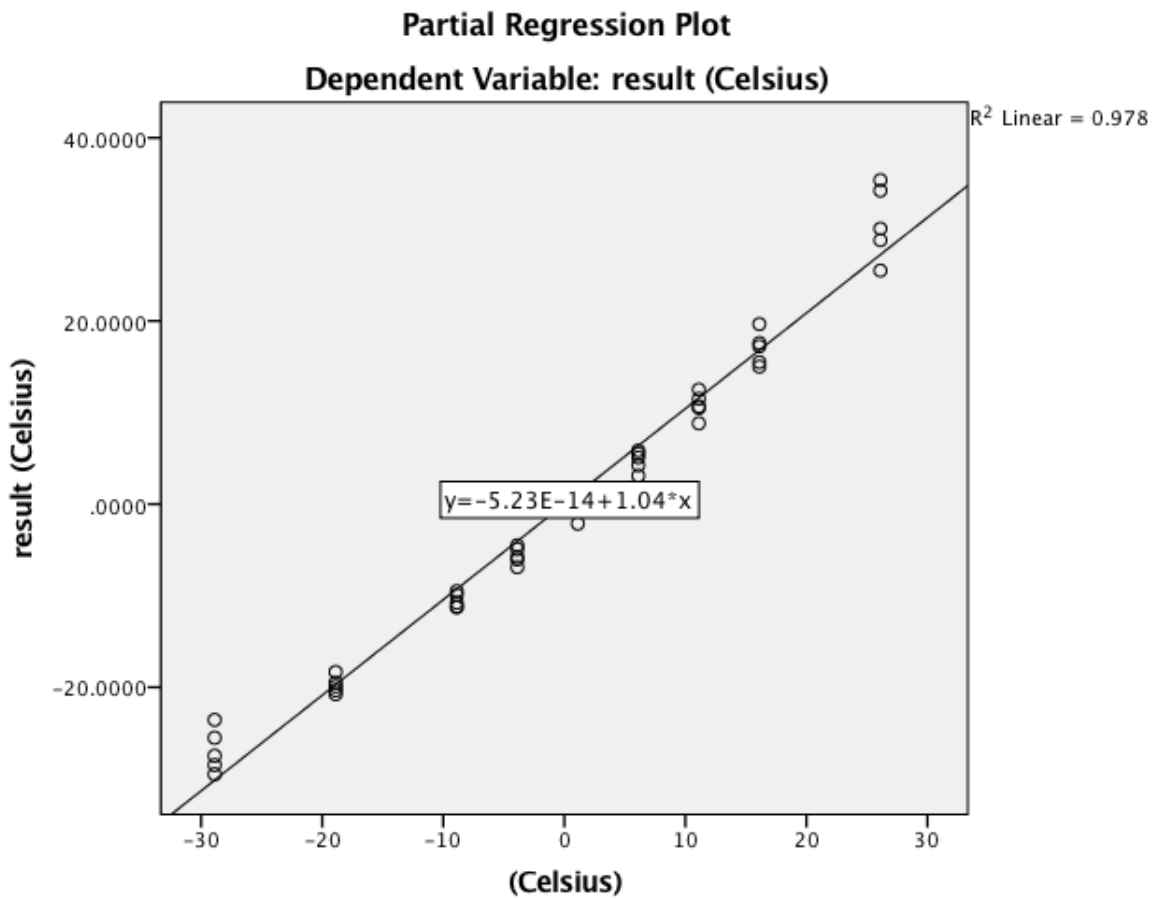


Figure 6.2: Partial Regression Plot of DV $T_{p,die}$ and IV T_b

It is obvious that the data points approximately fall to the line. The Correlation Coefficient R^2 is equal to 0.978 and so $R \approx 0.988$, which means that there is a very strong linear relationship between $T_{p,die}$ and T_b .

Assumption #2: Independence

A scatterplot of the Studentized Residuals versus the Cases the model has, is shown here:

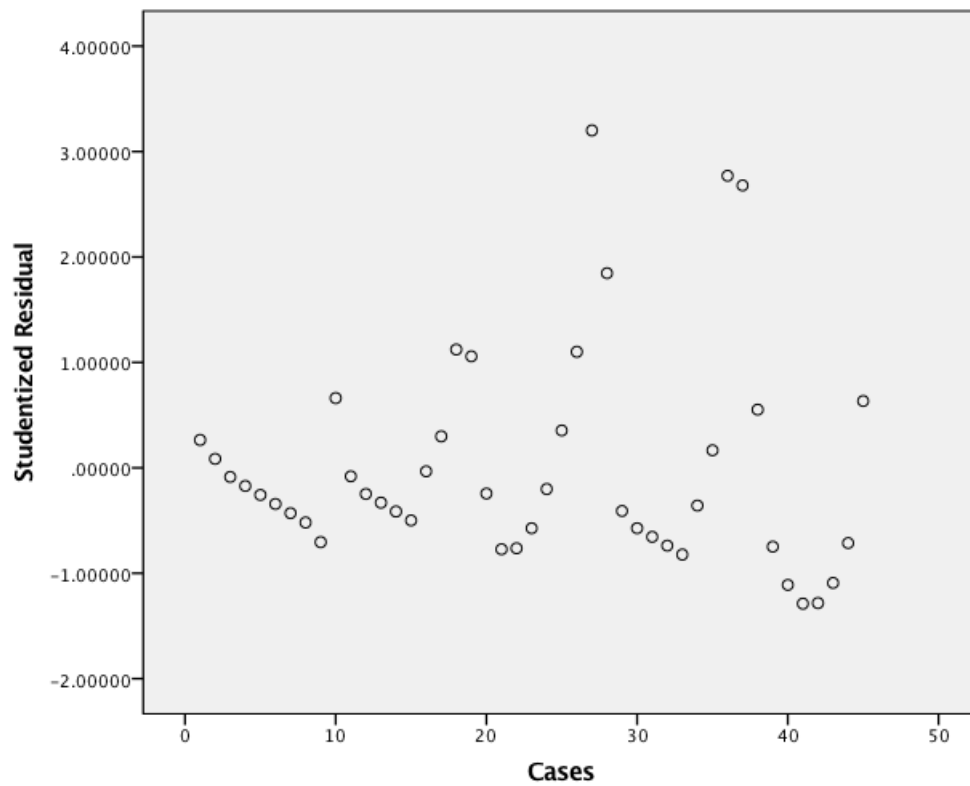


Figure 6.3: Scatterplot of the Studentized Residuals versus the Cases of the model

From this scatterplot I observe that the majority of the residuals are between $[-2,2]$ and are equally distributed to the X axis (where is Cases). This means residuals don't have a linear or non-linear relationship between them. So, there is independence between the data.

Assumption #3: Homoscedasticity

A scatterplot of the Studentized Deleted Residuals versus the Standardized Predicted Values the model has, is shown here:

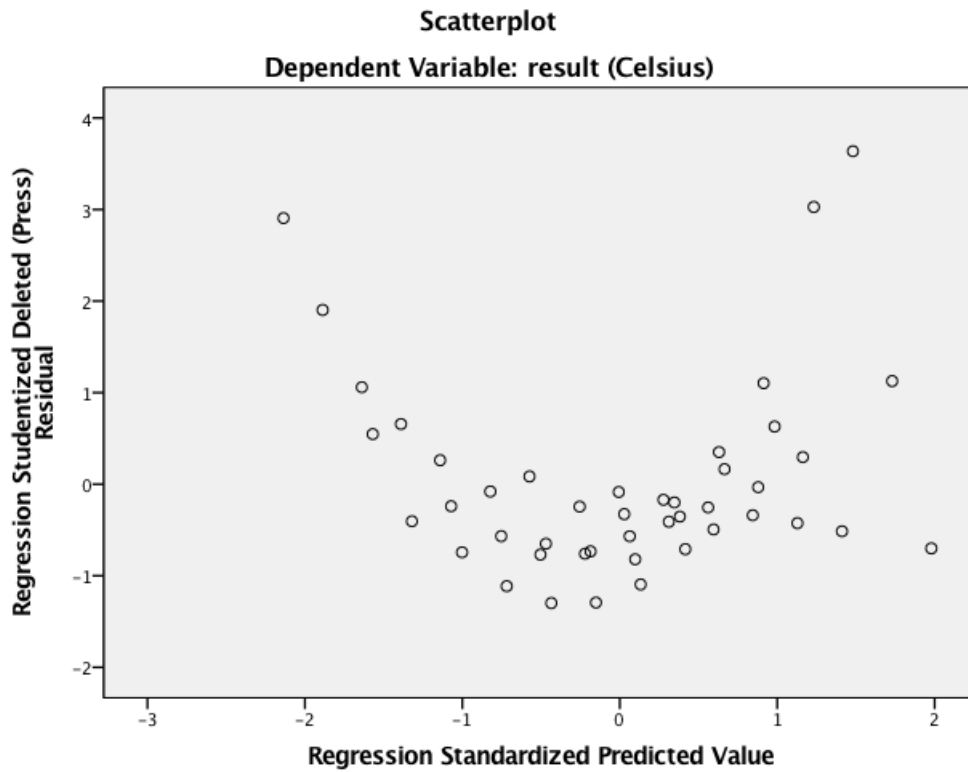


Figure 6.4: Scatterplot of the Studentized Deleted Residuals versus the Standardized Predicted Values of the model

From this scatterplot I observe that the majority of the residuals are again between $[-2,2]$ and are equally (randomly) distributed to the X axis through all the range of $T_{p,die}$ expected values. So, the model's data are homoscedastic.

Assumption #4: Normality

A histogram of the Regression Standardized Residuals and a Normal P-P Plot of Regression Standardized Residuals is shown here:

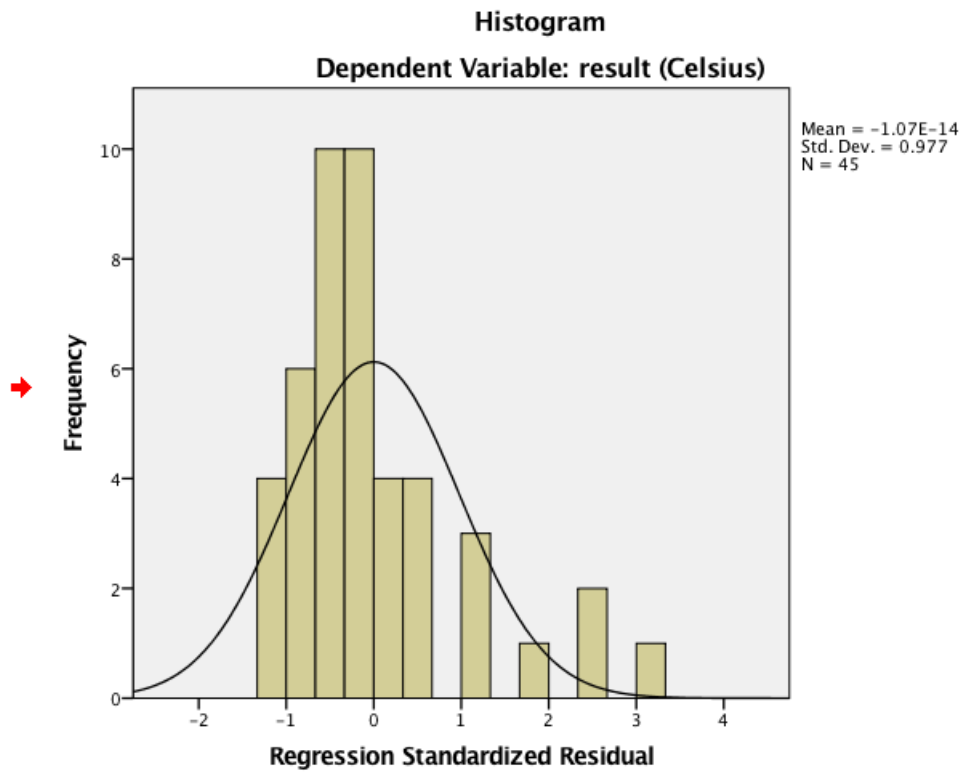


Figure 6.5: Histogram of the Regression Standardized Residuals

From Figure 6.5 I observe that there is satisfactory normality, with few exceptions. Most values are between $[-2,2]$, so there's not some extreme violation of normality here.

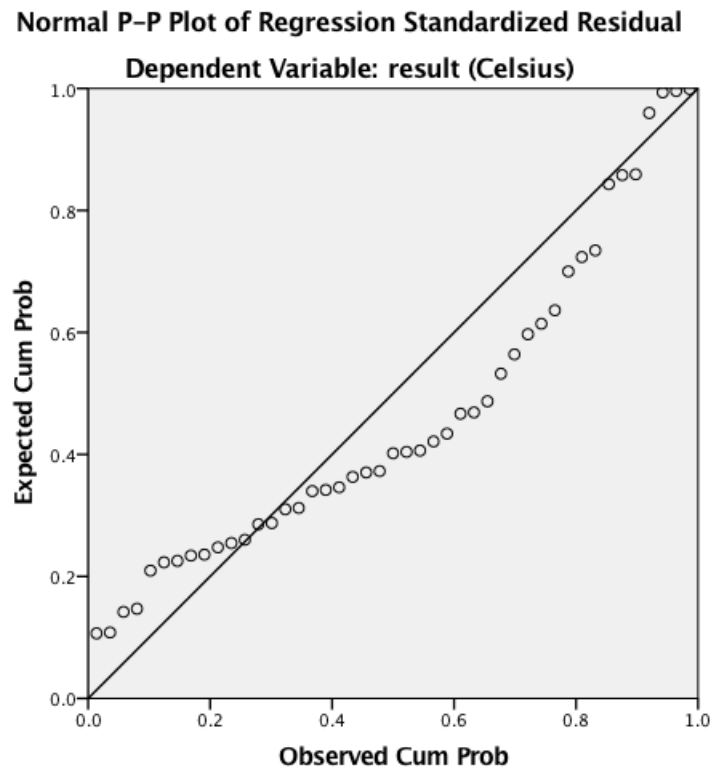


Figure 6.6: Normal P-P Plot of Regression Standardized Residuals

Figure 6.6 shows that the points are approximately close to the bisector of X and Y axis.

So, these 2 plots prove the normality of the model's data (approximately).

The assumptions of Multiple Linear Regression in this case are valid, so the equation of the MLR model can be found by interpreting some tables that SPSS produces.

Correlations				
		result (Celsius)	(rpm)	(Celsius)
Pearson Correlation	result (Celsius)	1.000	-.352	.925
	(rpm)	-.352	1.000	.000
	(Celsius)	.925	.000	1.000
Sig. (1-tailed)	result (Celsius)	.	.009	.000
	(rpm)	.009	.	.500
	(Celsius)	.000	.500	.
N	result (Celsius)	45	45	45
	(rpm)	45	45	45
	(Celsius)	45	45	45

Table 6.5: Correlations table containing *Pearson Correlation* for checking linearity of model's data, *Sig.(1-tailed)* for checking level of correlation between model's data and *N* for showing model's numbers of data

From Table 6.5, in *Pearson Correlation* line, both IVs (T_b and ω_{sc}) show strong correlation with DV ($T_{p,die}$). This shows again that there is linearity between the model's data.

Sig.(1-tailed) line shows again that correlations between the model's data are strong, as the significance level is below 0.5.

N shows the number of data inserted. So, as mentioned before, there are 45 cases in this model.

Model Summary^c

Model	R	R Square	Adjusted R Square	Std. Error of the Estimate	Change Statistics					Durbin-Watson
					R Square Change	F Change	df1	df2	Sig. F Change	
1	.925 ^a	.856	.853	7.1221259	.856	256.447	1	43	.000	
2	.990 ^b	.981	.980	2.6459634	.124	269.544	1	42	.000	.725

- a. Predictors: (Constant), (Celsius)
- b. Predictors: (Constant), (Celsius), (rpm)
- c. Dependent Variable: result (Celsius)

Table 6.6: Model Summary table containing: R^2 (*R square*) which shows the proportion of the variance for the dependent variable that is explained by the independent variables (goodness of fit indicator), R which is the square root of R square, *Adjusted R Square* which is a modified version of R-squared for the number of predictors in the model, *R Square Change* which is just the change in R-square when a new predictor is added and *Durbin-Watson* indicator which is used for proving independence between the predictors

From Table 6.6, the R Square value (R^2) of 0.981 indicates that 98.1% of the variation in $T_{p,die}$ can be explained by the model containing T_b and ω_{sc} . This is pretty high, so predictions from the regression equation are fairly reliable.

Coefficients^a

Model		Unstandardized Coefficients		Standardized Coefficients	t	Sig.	Collinearity Statistics	
		B	Std. Error	Beta			Tolerance	VIF
1	(Constant)	-28.089	14.304		-1.964	.056	1.000	1.000
	(Celsius)	1.044	.065	.925	16.014	.000		
2	(Constant)	-16.641	5.360		-3.105	.003	1.000	1.000
	(Celsius)	1.044	.024	.925	43.105	.000		
	(rpm)	-.229	.014	-.352	-16.418	.000		

- a. Dependent Variable: result (Celsius)

Table 6.7: Coefficients table containing: B column showing the coefficients of the Multiple Linear Regression model, t values showing the contribution of each variable to the model, Sig column which shows the significance of each variable to the model, *Tolerance* and *VIF* which show collinearity problems

Something not mentioned to the Assumptions before is:

Assumption #5: No or little Multicollinearity

Columns *Tolerance* and *VIF* from Table 6.7 help to prove this assumption.

Tolerance shows **tolerance factor** (a number between 0 and 1 which shows the percentage of variance of each IV). There is a problem if that number is below 0.1, something that doesn't happen here. VIF (**Variance Inflation Factor**) indicates there is a multicollinearity problem if its value is above 10, something that doesn't happen here for all the IV.

So multicollinearity is not a problem for this MLR model and the model's equation can be found from this Table.

B column in the coefficients table, gives us the coefficients for each independent variable in the regression model. So the equation for MLR model is:

$$T_{p,die} = -16.641 + 1.044 * T_b - 0.229 * \omega_{sc} \quad (6.6)$$

Last but not least, t column shows the significance for each variable in the MLR model. Variable T_b is the **best predictor variable** and then follows ω_{sc} .

Chapter 7

Mathematical Modeling of the Single Screw Extruder Profile using ANFIS and comparing with other Mathematical Models

In this chapter an adaptive neuro-fuzzy inference system (ANFIS) model (which is a combination of neural network and fuzzy logic as described in 5.12) was evaluated to predict the Single Screw Extruder Profile by creating 2 models: a Die Melt Temperature Model (T_4) and a Screw Speed Model (ω_{sc}). ANFIS models were compared with the corresponding Arrhenius models (created them by following exactly the same steps as I did in 6.2.1). New data set was used for the creation of these models.

7.1 Experimental Inputs for the Models Creation

Checking the number of data used in Chapter 6, it's obvious that they are not enough for the training/testing sets required for models creation and evaluation. For this reason, I also used a data set from ([Abeykoon, Li, Martin, & Kelly, 2011](#)) to create and compare models.

All measurements were carried out on a 63.5mm diameter (D) single screw extruder (Davis Standard BC-60). A tapered gradual compression (GC) screw (with 3:1 compression ratio) was used to process material and details are shown in Figure 7.1.

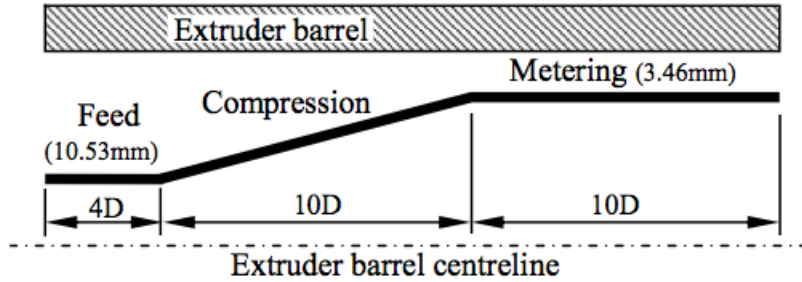


Figure 7.1: Details of the GC screw

Experimental trials were carried out on a virgin high density polyethylene (HDPE), (ExxonMobil HYA 800), (density: $0.961\text{g}/\text{cm}^3$, melt flow index (MFI): $0.7\text{g}/10\text{min}$ @ ($190\text{ }^\circ\text{C}$, 2.16kg)). The extruder temperature settings were fixed as described in Table 7.1 under three different barrel set temperature conditions and denoted as A (high temperature), B (medium temperature) and C (low temperature).

Temperature settings	Set temperatures ($^\circ\text{C}$)						
	Barrel zones				Clamp ring	Adapter	Die
	1	2	3	4			
A	110	130	180	230	230	230	230
B	105	125	175	215	215	215	215
C	100	120	170	200	200	200	200

Table 7.1: Extruder barrel temperature settings

Experiments were started with temperature setting A and data was recorded with the screw stationary for 1 minute. Then, the screw speed was increased up to 90rpm with random steps of between ± 5 and 40rpm and for the different barrel set temperatures with the extruder running for about 151 and 193 minutes continuously. The extruder was allowed to stabilise over 15 minutes after each set temperature change whereas it was running for about 7 minutes over each of the other different conditions. All of these settings were selected in order to generate realistic processing conditions whilst covering the full operating range of the extruder (i.e. 0-100rpm).

The data set from (Abeykoon, Li, Martin, & Kelly, 2011) contains 760 values of 5 variables (ω_{sc} , T_1 , T_2 , T_3 , T_4). As I mentioned in the beginning of this chapter, in order to model the Single Screw Extruder Profile I created 2 different models:

- **Die Melt Temperature Model:** The melt temperature profile at the die can be represented as a function of ω_{sc} , T_b :

$$T_{p,die} = f(\omega_{sc}, T_b) \quad (7.1)$$

where $T_{p,die}$ is actually T_4 , ω_{sc} is the screw speed and T_b represents the barrel set temperatures at different zones (T_1 , T_2 , T_3).

- **Screw Speed Model:** The screw speed can be represented as a function of $T_{p,die}$, T_b :

$$\omega_{sc} = f(T_{p,die}, T_b) \quad (7.2)$$

where $T_{p,die}$ is actually T_4 and T_b represents the barrel set temperatures at different zones (T_1 , T_2 , T_3).

7.2 Statistical Verification of the Models

In order to test the ANFIS and Arrhenius models accuracy, some graphic plots and common metrics were used. The metrics are:

- **ME** (Modeling Errors)

$$ME = y_i(t) - \hat{y}_i(t) \quad (7.3)$$

Here, I use modeling errors in a plot between real testing values and model estimated prices, in order to show the model's capability of parameter estimation to capture the physical behavior of the structure.

- **RMSE** (Root Mean Square Errors)

$$RMSE = \sqrt{\frac{1}{N} \sum_{i=1}^N [(\hat{y}_i(t) - y_i(t))]^2} \quad (7.4)$$

RMSE describes the average difference between predicted values and model measured values.

- r^2 (Squared Residuals)

$$r_i^2 = (y_i(t) - \hat{y}_i(t))^2 \quad (7.5)$$

r represents the degree of association between the predicted and the model measured values.

- **MAD** (Mean Absolute Deviation)

$$MAD = \frac{1}{n} \sum_{i=1}^n |x_i - \bar{x}| \quad (7.6)$$

The Mean Absolute Deviation (MAD) of a set of data is the average distance between each data value and the mean.

- **MAPE** (Mean Absolute Percentage Error)

$$MAPE = \frac{100\%}{n} \sum_{t=1}^n \left| \frac{A_t - B_t}{A_t} \right| \quad (7.7)$$

MAPE is the average absolute percent error for each forecast minus actuals divided by actuals. It's a regression quality measure and expresses accuracy as a percentage.

7.3 Die Melt Temperature Profile Modeling and Verification

7.3.1 Arrhenius Model based on Linear Least Squares Regression and Verification

The matlab script gave these results:

$$\mathbf{E}/\mathbf{R} = 742,6639$$

$$\mathbf{k}_0 = 617,177$$

$$\mathbf{n} = -0.0035$$

So, the die melt temperature profile model based on Arrhenius model and Linear Least Squares Regression is:

$$T_{p,die} = 617.177 * e^{-742.6639 * T_b} * \omega_{sc}^{-0.0035} \quad (7.8)$$

For the verification part, in Figure 7.3 the real testing values vs the model estimated values for the same t (min) values are depicted.

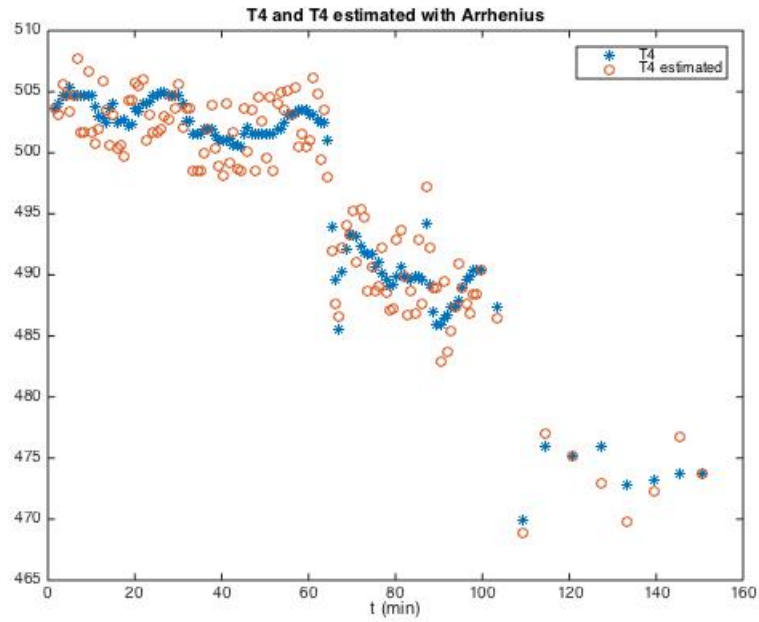


Figure 7.2: Original vs Model Estimated prices of the melt temperature profile at the die (T_4)

The model prediction errors of the selected Arrhenius model on the unseen testing data for the melt temperature profile at the die (T_4) is shown in Figure 7.4. It is obvious that modeling errors are in a range of $[-3,+3]$

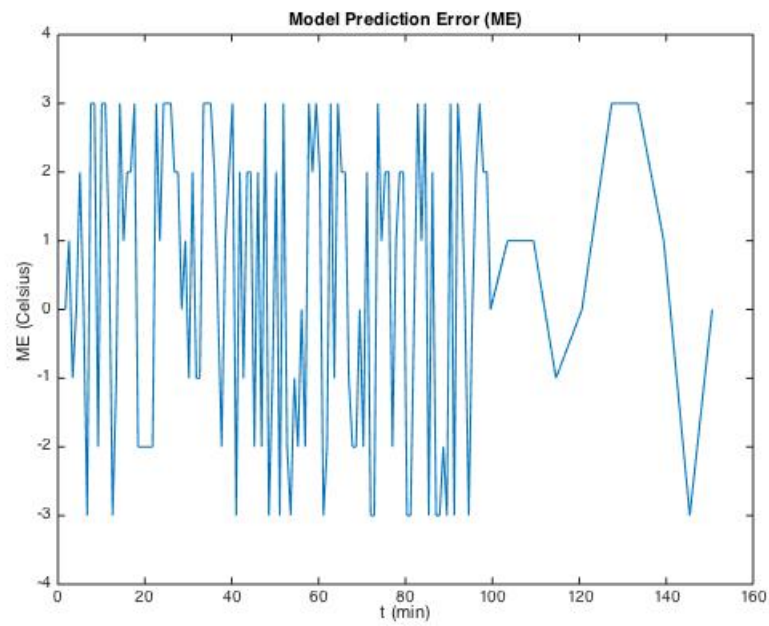


Figure 7.3: Performance of the Arrhenius model for the melt temperature profile at the die (T_4) with the model prediction error (ME)

The common metric results based on the testing and model estimated values are:

$$\text{RMSE} = 2.2041454009$$

$$\text{MAD} = 1.97637904$$

$$\text{MAPE} = 0.3978208485 \%$$

7.3.2 ANFIS Verification Results

In Figure 7.7 the real testing values vs the model estimated values for the same t (min) values are depicted.

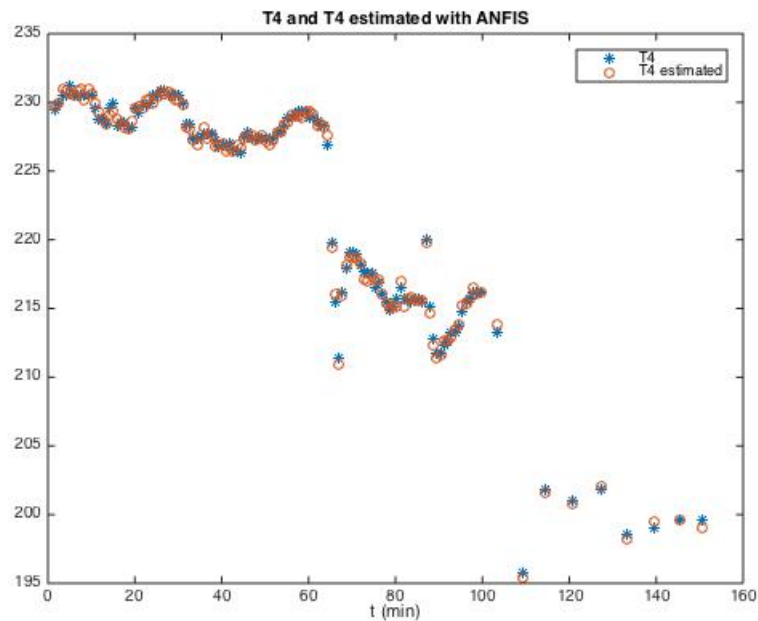


Figure 7.4: Original vs Model-Estimated prices of the melt temperature profile at the die (T_4)

The model prediction errors of the selected ANFIS model on the unseen testing data for the melt temperature profile at the die (T_4) is shown in Figure 7.8. It is obvious that modeling errors are in a range of $[-0.5,+0.5]$

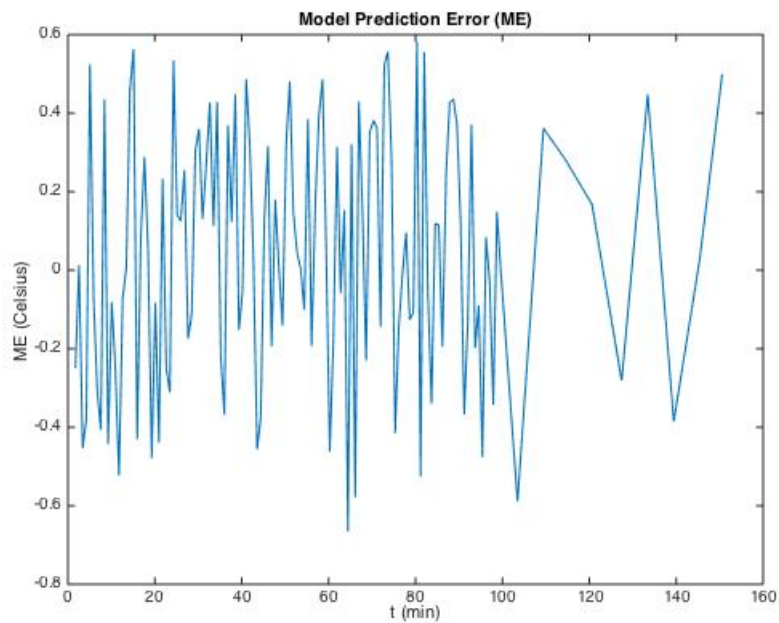


Figure 7.5: Performance of the ANFIS model for the melt temperature profile at the die (T_4) with the model prediction error (ME)

The common metric results based on the testing and model estimated values are:

$$\text{RMSE} = 0.3220907428$$

$$\text{MAD} = 0.0019667049$$

$$\text{MAPE} = 0.1235688931 \%$$

7.3.3 Comparison of Arrhenius and ANFIS model

Checking Figure 7.2 with Figure 7.4 (which contain the Original vs Model estimated prices of the melt temperature profile at the die) I see that ANFIS estimated prices are a lot closer to the real testing values than those estimated from the Arrhenius model.

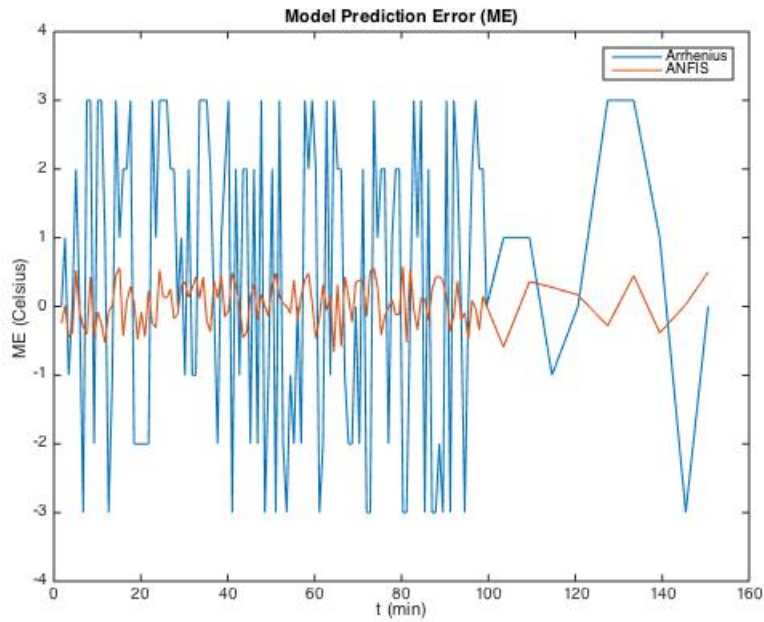


Figure 7.6: Performance of both models for the melt temperature profile at the die (T_4) with the model prediction error (ME)

This is also obvious from Figure 7.6 (Model Prediction Error figure), where for Arrhenius the modeling errors are in a range of $[-3,+3]$ while for ANFIS the modeling errors are in a much smaller range of $[-0.5,+0.5]$.

In Table 7.2 I give the common metric results for both Arrhenius and ANFIS model, as seen above.

	Arrhenius	ANFIS
RMSE	2.2041454009	0.3220907428
MAD	1.97637904	0.0019667049
MAPE (%)	0.3978208485	0.1235688931

Table 7.2: Common metric results for the melt temperature profile at the die (T_4) between Arrhenius and ANFIS model

These results confirm the previous conclusion that ANFIS predicts the actual testing values of the die melt temperature profile with much more accuracy compared to Arrhenius.

7.4 Screw Speed Modeling and Verification

7.4.1 Arrhenius Model based on Linear Least Squares Regression and Verification

The matlab script gave these results:

$$\mathbf{E}/\mathbf{R} = 373,31$$

$$\mathbf{k}_0 = 2300,8$$

$$\mathbf{n} = -0.004$$

So, the screw speed profile model based on Arrhenius model and Linear Least Squares Regression is:

$$\omega_{sc} = 2300.8 * e^{-373.31 * T_{p,die}} * T_b^{-0.004} \quad (7.9)$$

For the verification part, in Figure 7.5 the real testing values vs the model estimated values for the same t (min) values are depicted.

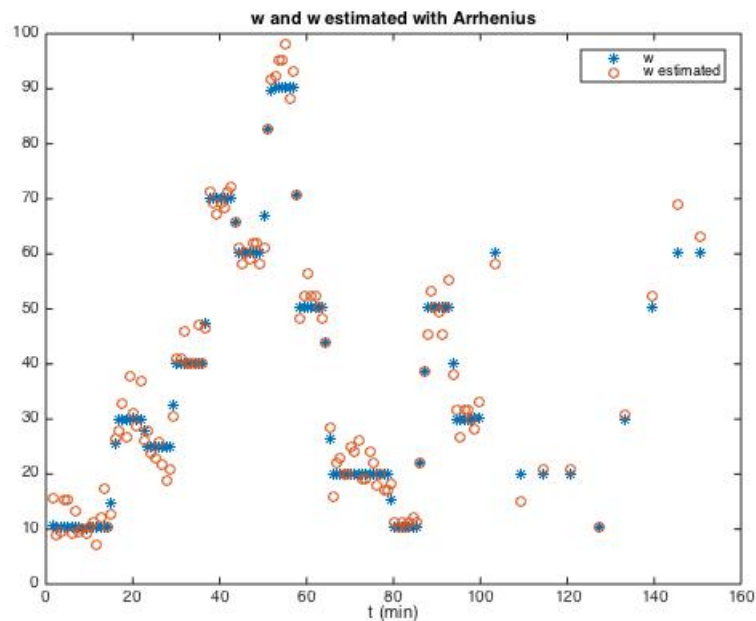


Figure 7.7: Original vs Model-Estimated prices of the screw speed (ω_{sc})

The model prediction errors of the selected Arrhenius model on the unseen testing data for the screw speed (ω_{sc}) is shown in Figure 7.6. It is obvious that modeling errors are in a range of $[-10,+6]$

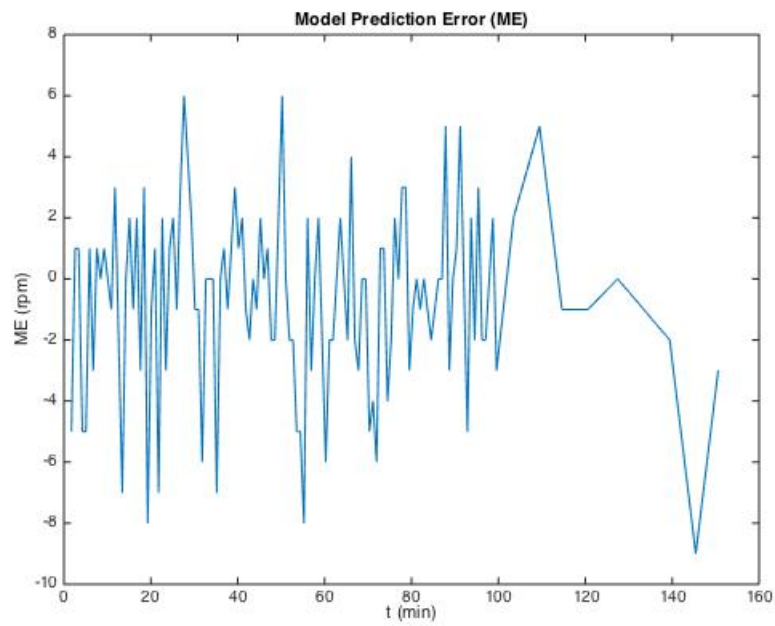


Figure 7.8: Performance of the Arrhenius model for the screw speed (ω_{sc}) with the model prediction error (ME)

The common metric results based on the testing and model estimated values are:

$$\text{RMSE} = 3.0117904756$$

$$\text{MAD} = 5.39370327$$

$$\text{MAPE} = 8.8848578998 \%$$

7.4.2 ANFIS Verification Results

In Figure 7.9 the real testing values vs the model estimated values for the same t (min) values are depicted.

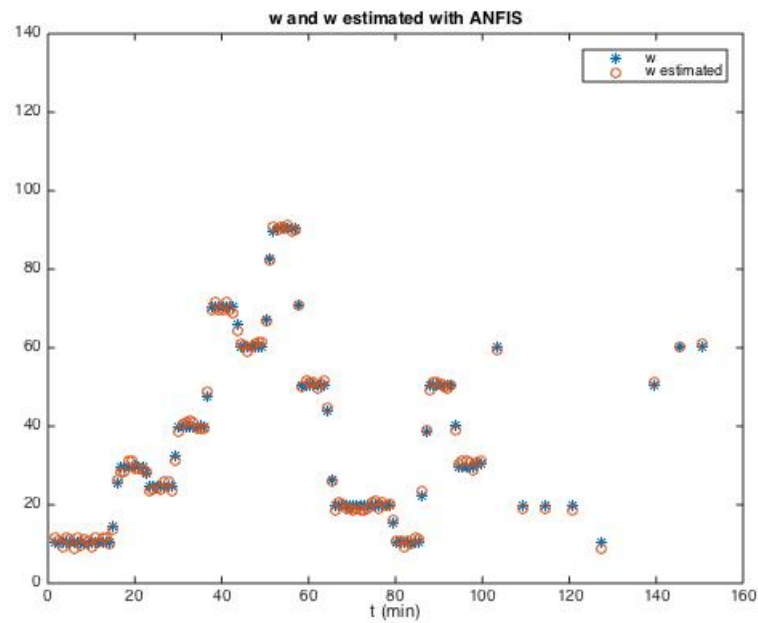


Figure 7.9: Original vs Model-Estimated prices of the screw speed (ω_{sc})

The model prediction errors of the selected ANFIS model on the unseen testing data for the screw speed (ω_{sc}) is shown in Figure 7.10. It is obvious that modeling errors are in a range of $[-1.5,+1.5]$

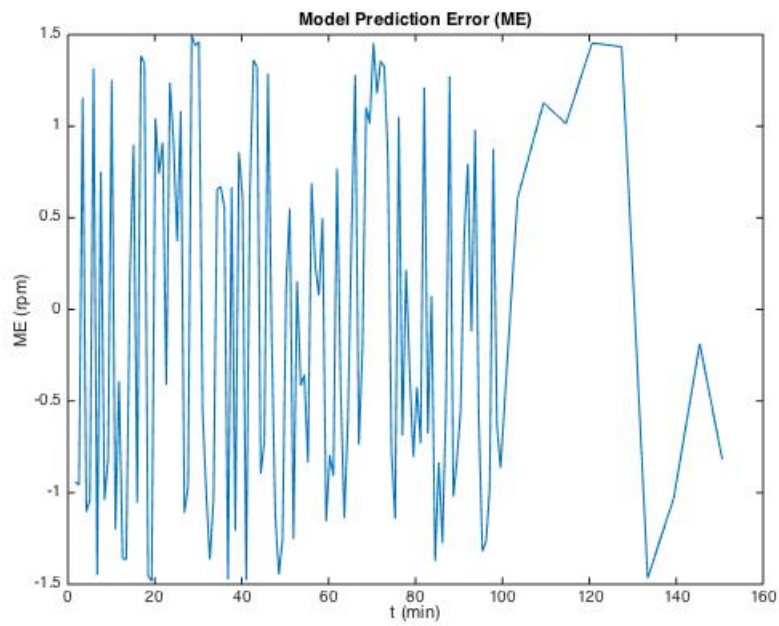


Figure 7.10: Performance of the ANFIS model for the screw speed (ω_{sc}) with the model prediction error (ME)

The common metric results based on the testing and model estimated values are:

$$\text{RMSE} = 0.9866420453$$

$$\text{MAD} = 0.0074011099$$

$$\text{MAPE} = 3.9880881043 \%$$

7.4.3 Comparison of Arrhenius and ANFIS model

Checking Figure 7.7 with Figure 7.9 (which contain the Original vs Model estimated prices of the screw speed) I see that ANFIS estimated prices are a lot closer to the real testing values than those estimated from the Arrhenius model.

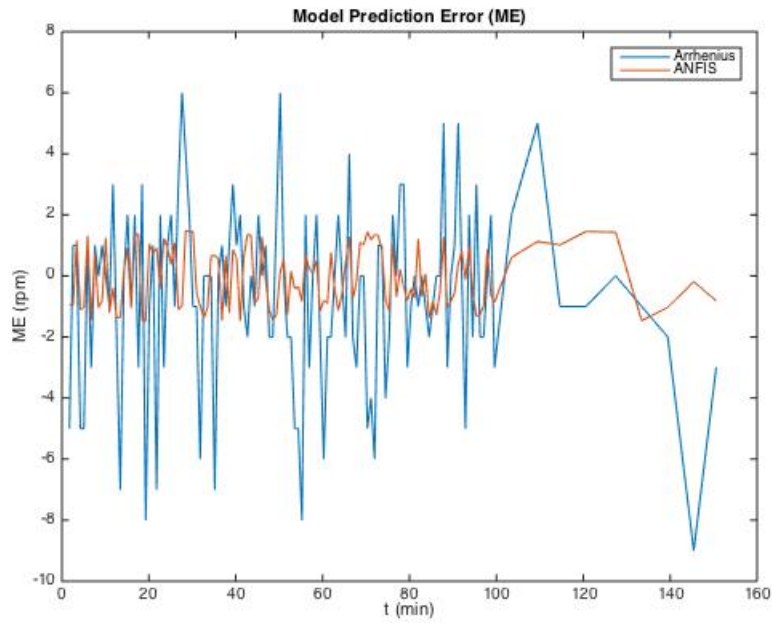


Figure 7.11: Performance of both models for the screw speed (ω_{sc}) with the model prediction error (ME)

This is also obvious from Figure 7.11 (Model Prediction Error figure), where for Arrhenius the modeling errors are in a range of $[-10,+6]$ while for ANFIS the modeling errors are in a much smaller range of $[-1.5,+1.5]$.

In Table 7.3 I give the common metric results for both Arrhenius and ANFIS model, as seen above.

	Arrhenius	ANFIS
RMSE	3.0117904756	0.9866420453
MAD	5.39370327	0.0074011099
MAPE (%)	8.8848578998	3.9880881043

Table 7.3: Common metric results for the screw speed (ω_{sc}) between Arrhenius and ANFIS model

These results confirm the previous conclusion that ANFIS predicts the actual testing values of the screw speed with much more accuracy compared to Arrhenius.

7.5 Final Single Screw Extruder Profile model

Our goal is to find every time the right value of ω_{ref} as an input to the extruder for a good result. As seen in 7.4.3 ANFIS predicts more accurate screw speed testing values. So with the help of ANFIS for the ω_{sc} model we can achieve the desired ω_{ref} , as seen in Figure 7.12

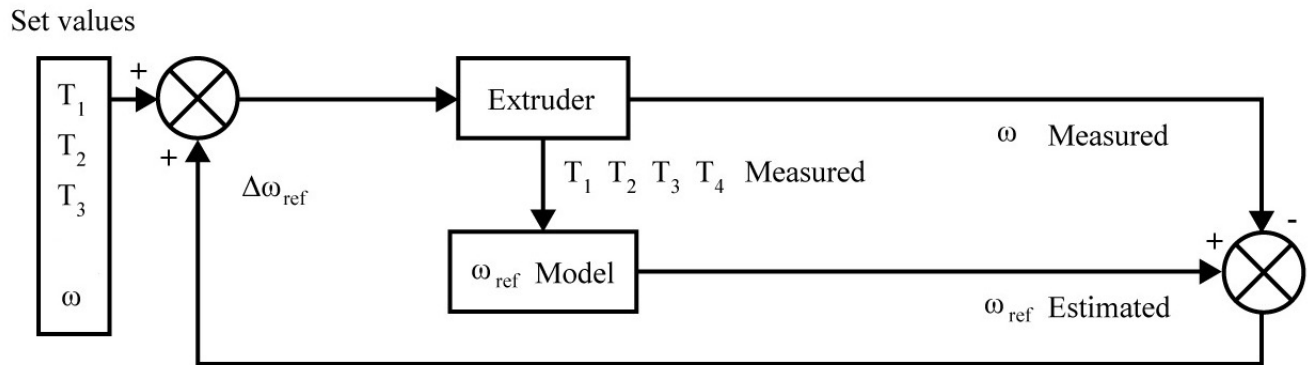


Figure 7.12: Proposed Single Screw Extrusion Profile model

The model firstly puts the set values to the extruder (T_1 , T_2 , T_3 , T_4 , ω). Then, the measured temperature values from the extruder get as an input to the ω_{ref} model. After that, the difference from the actual screw speed from the extruder ($\omega_{measured}$) and the screw speed from the ω_{ref} model ($\omega_{ref_estimated}$) is estimated. This difference ($\Delta\omega_{ref}$) is used to set the right ω speed to the Extruder for the optimal result.

The proposed model has online adaptability. This means, the controller determines the average screw speed based on the actual effects of process settings (i.e. screw speed and barrel set temperatures), materials, and machine geometry. With this way the process maintains stable while ensuring process safety.

Chapter 8

Conclusions and Future Work

8.1 Conclusions

A novel fuzzy approach to solve “automatically” single screw extrusion inverse problems was proposed and implemented in this work. The scheme developed was applied to the setting of the optimal operating conditions of an existing extruder with real training/testing values.

Fuzzy controllers are of easy application, show the capacity to deal with complex search spaces, do not require any sort of additional information and the results are sensitive to the process parameters with physical meaning. Furthermore, fuzzy controllers can be changed to take into account the existence of several criteria to be satisfied simultaneously, which is a characteristic of most real world optimisation problems

So, a model-based fuzzy control framework to reduce the die melt temperature variance while achieving the desired average die melt temperature was proposed and the simulation results confirmed its efficacy. The controller determines the average screw speed based on a radial temperature profile of the die melt flow rather than a point-based measurement which is less accurate although common in practice. Proposed fuzzy controller system provides good control capabilities to maintain the melt temperature homogeneity within desired limits by manipulating screw speed and barrel set temperatures in parallel. The controller performances can be further improved by improving the models accuracies etc. Therefore, this may offer a new method to operate extruders at high screw speeds whilst achieving both high energy and thermal efficiencies.

8.2 Future Work

Knowledge-based fuzzy rules were not implemented in this work, so adding them should be carried out. Development of generalised models should enable use of the controller with different materials and machine geometries and will be addressed under future work. Also, the implementation of the proposed controller on different extruders should be carried out to evaluate its performance.

References

- Abeykoon, C., Kelly, A. L., Martin, P. J., & Li, K. (2013). Dynamic modelling of die melt temperature profile in polymer extrusion. In *Decision and control (cdc), 2013 ieee 52nd annual conference on* (pp. 2550–2555). [2](#), [10](#), [13](#), [14](#)
- Abeykoon, C., Li, K., Martin, P. J., & Kelly, A. L. (2011). Modelling of melt pressure development in polymer extrusion: Effects of process settings and screw geometry. In *Modelling, identification and control (icmic), proceedings of 2011 international conference on* (pp. 197–202). [70](#), [72](#)
- Abeykoon, C., Li, K., McAfee, M., Martin, P. J., & Irwin, G. W. (2011). Extruder melt temperature control with fuzzy logic. *IFAC Proceedings Volumes*, *44*(1), 8577–8582. [6](#)
- Abeykoon, C., Li, K., McAfee, M., Martin, P. J., Niu, Q., Kelly, A. L., & Deng, J. (2011). A new model based approach for the prediction and optimisation of thermal homogeneity in single screw extrusion. *Control Engineering Practice*, *19*(8), 862–874. [13](#), [20](#), [22](#), [23](#), [33](#), [36](#)
- Abeykoon, C., McAfee, M., Li, K., Kelly, A., & Brown, E. (2010). Monitoring the effect of operating conditions on melt temperature homogeneity in single-screw extrusion. *SPE ANTEC technical papers*, *1*, 1799–806. [21](#), [55](#), [56](#)
- Anger, K., Potente, H., Schöppner, V., Enns, E., et al. (2009). Dynamic temperature and pressure measurement in polymer processing. *Journal of Plastics Technology*, *5*(1), 31. [21](#), [23](#), [24](#), [25](#), [26](#)
- AZoMaterials. (2009). The importance of intrinsic viscosity (iv) measurement throughout the pet supply chain - lloyd instruments. (IV and PET) [27](#)
- Bhatia, A., & Yu-Wei, C. D. C. (2017). *Machine learning with r cookbook: Analyze data and build predictive models*. Packt Publishing Ltd. [43](#), [47](#), [53](#)
- Bur, A. J., & Roth, S. C. (2004). Fluorescence temperature measurements: Methodology for applications to process monitoring. *Polymer Engineering & Science*, *44*(5), 898–908. [21](#), [24](#)

- Deng, J., Li, K., Harkin-Jones, E., Price, M., Karnachi, N., Kelly, A., ... Fei, M. (2014). Energy monitoring and quality control of a single screw extruder. *Applied Energy*, *113*, 1775–1785. [4](#), [5](#), [6](#), [7](#), [11](#), [12](#), [13](#)
- Elhami, B., Akram, A., Khanali, M., & Mousavi-Avval, S. H. (2016). Application of anfis and linear regression models to analyze the energy and economics of lentil and chickpea production in iran. *Energy Equipment and Systems*, *4*(2), 255–270. [54](#)
- Geissler, T. (2006). Investigation of the flow characteristics of pet at different temperatures. *Thermo Fisher Scientific*. [11](#), [13](#)
- Jang, J.-S. (1993). Anfis: adaptive-network-based fuzzy inference system. *IEEE transactions on systems, man, and cybernetics*, *23*(3), 665–685. [53](#)
- Kelly, A., Brown, E., Howell, K., & Coates, P. (2008). Melt temperature field measurements in extrusion using thermocouple meshes. *Plastics, Rubber and Composites*, *37*(2-4), 151–157. [2](#), [21](#), [22](#), [24](#)
- Kuhn, M., & Johnson, K. (2013). *Applied predictive modeling* (Vol. 26). Springer. [46](#)
- Li, K., & Martin, P. (2010). An integrated system of inferential measurement and control of polymer extrusion for self-tuning optimisation and response to disturbances. [9](#)
- Liang, J., Li, R., & Tjong, S. (1999). Effects of pressure and temperature on the melt density and the melt flow rate of ldep and glass bead-filled ldpe composite. *Journal of Materials Processing Technology*, *91*(1-3), 167–171. [28](#)
- Liu, X., Li, K., McAfee, M., Nguyen, B. K., & McNally, G. M. (2012). Dynamic gray-box modeling for on-line monitoring of polymer extrusion viscosity. *Polymer Engineering & Science*, *52*(6), 1332–1341. [8](#), [10](#)
- PCA. (n.d.). *Principal component analysis — Wikipedia, the free encyclopedia*. Retrieved from https://en.wikipedia.org/wiki/Principal_component_analysis [50](#)
- Rasid, R., & Wood, A. (2003). Effect of process variables on melt temperature profiles in extrusion process using single screw plastics extruder. *Plastics, rubber and composites*, *32*(5), 187–192. [13](#)
- Reiloy. (2015). Barrel and screw handbook [Computer software manual]. (Screw manual) [17](#)
- Sanjabi, F. (2010). *Helical flow of polymer melts in extruders: Model development and validation with experiments* (Vol. 72) (No. 05). [9](#), [11](#), [12](#), [19](#), [27](#), [29](#), [37](#), [39](#), [41](#)
- Vera-Sorroche, J., Kelly, A. L., Brown, E. C., Gough, T., Abeykoon, C., Coates, P. D., ... Price, M. (2014). The effect of melt viscosity on

- thermal efficiency for single screw extrusion of hdpe. *Chemical Engineering Research and Design*, 92(11), 2404–2412. [18](#)
- Williams, B. (2017). *Biostatistics: Concepts and applications for biologists*. CRC Press. [51](#)
- Wood, A., & Rasid, R. (2003). Effect of process variables on melt velocity profiles in extrusion process using single screw plastics extruder. *Plastics, rubber and composites*, 32(5), 193–198. [20](#)

Appendix A

A.1 HDPE - B4020N1343



Product Technical Information

Eltex® B4020N1343 is a high-density polyethylene copolymer particularly intended for the injection moulding and compression moulding of screw caps for the packaging of beverages. It is especially suitable for applications requiring high environmental stress cracking resistance. Thanks to high purity and excellent organoleptic properties, this grade is particularly intended for the packaging in direct contact with beverages

Typical applications

- Caps & closures for the packaging of sparkling water and carbonated soft drinks

Benefits and Features

- Very good stress cracking resistance
- Excellent processing performances
- High impact strength
- Excellent, quality controlled organoleptic properties. . In order to preserve the excellent organoleptic properties, it is important not to exceed a melt temperature of 250°C during processing.
- Grade containing slip agent ensuring easy application and opening
Exposure to direct sunlight has to be avoided as the slip agent is light sensitive and its degradation can give off-taste to the beverage.

Properties		Test Methods	Values	Units
Physical				
Density		ISO 1872	952	kg/m ³
Melt Flow Rate	2.16 kg load	ISO 1133	2.2	g/10min
Mechanical				
Tensile Modulus		ISO 527 -1&2 (1B)	1100	MPa
Tensile Strength	@ Yield	ISO 527 -1&2 (1B)	25	MPa
Charpy Impact Strength, 23°C		ISO 179	6	kJ/m ²
Environmental Stress Cracking Resistance (ESCR)		INEOS	16	h
Other				
Organoleptic properties		INEOS	OK	-

September, 2007

Published by
INEOS Polyolefins

A.2 PET

Polyester Resin from **INVISTA**

Polyclear® Refresh PET 1101

Product Description

Polyclear® Refresh PET 1101 is a copolymer packaging resin with a nominal intrinsic viscosity of 0.83 dl/g. Packaging made from Polyclear® Refresh PET 1101 has excellent clarity and is noted for its dimensional stability, which prevents shrinkage and expansion of the container. Polyclear® Refresh PET 1101 is used successfully in carbonated soft drink bottles and other applications such as water bottles, food containers, and packaging for household goods.

This polymer complies with the Federal Food, Drug, and Cosmetic Act for certain food contact applications. Please contact INVISTA for specific FDA clearances.

Polyclear® Refresh PET 1101 offers excellent performance in maximum throughput, stretch-blow molding applications. Preforms made from Polyclear® Refresh PET 1101 allow maximum blowing throughputs by quickly heating in the infrared (IR) ovens. In addition, bottles made from Polyclear® Refresh PET 1101 are low-stick, which eases handling issues.

Containers made from INVISTA PET are lightweight, have excellent clarity, and are shatterproof. With the important advantage of being totally recyclable, PET is the packaging material of choice.

Property	Value	Test Method
General		
Intrinsic Viscosity*	0.83 ± 0.02	1% Solution in Dichloroacetic Acid*
Melting Point (°C)	252 Maximum	DSC**
Carboxyl End Groups (meq/kg)	45 Maximum	Titration**
Diethylene Glycol Content (wt%)	1.8 Maximum	Gas Chromatography**
Acetaldehyde Content (ppm)	2.0 Maximum	Gas Chromatography**
Density (g/ cm ³)	1.39 Minimum	Pycnometer
Fines (%)	0.05 (through 28 mesh)	Gravimetric determination as manufactured
Moisture Content (%)	0.1 Maximum	Karl Fisher Titration as manufactured
Crystallinity (%)	50 Minimum	Pycnometer
Bulk Density (packed) lb/ ft ³	52 Minimum	***
Chip Size (grams / 100 chips)	2.0 Maximum	

* Determined by conversion of solution viscosity to intrinsic viscosity using an empirical correlation developed by INVISTA equivalent to ASTM method D-4603.

** Internal method

*** Not equivalent to bulk density found with fully packed, larger quantities.

INVISTA S.à r.l.
Polymer and PET Resins Business
4235 S. Stream Blvd
One Lake Pointe Plaza
Charlotte, NC 28217

Issue Date: April 30, 2010

Additional Information:
<http://polymers.INVISTA.com/contact>

Typical
Property
Data Sheet

Revision # 8